

# Airborne measurements of new particle formation in the free troposphere above the Mediterranean Sea during the HYMEX campaign

C. Rose<sup>1</sup>, K. Sellegri<sup>1</sup>, E. Freney<sup>1</sup>, R. Dupuy<sup>1</sup>, A. Colomb<sup>1</sup>, J.-M. Pichon<sup>1</sup>, M. Ribeiro<sup>1</sup>, T. Bourianne<sup>2</sup>, F. Burnet<sup>2</sup>, and A. Schwarzenboeck<sup>1</sup>

[1]{Laboratoire de Météorologie Physique CNRS UMR6016, Observatoire de Physique du Globe de Clermont-Ferrand, Université Blaise Pascal, France}

[2]{Centre National de Recherches Météorologiques - Groupe d'étude de l'Atmosphère Météorologique, Météo France/CNRS, Toulouse, France}

## Abstract

While atmospheric new particle formation (NPF) has been observed in various environments and was found to contribute significantly to the total aerosol particle concentration, the production of new particles over open seas is poorly documented in the literature. Nucleation events were detected and analysed over the Mediterranean Sea using two condensation particle counters and a Scanning Mobility Particle Sizer on-board the ATR-42 research aircraft during flights conducted between the 11<sup>th</sup> of September and the 4<sup>th</sup> of November 2012 in the framework of the HYMEX (HYdrological cycle in Mediterranean EXperiment) project. The main purpose of the present work was to characterize the spatial extent of the NPF process, both horizontal and vertical. Our findings show that nucleation is occurring over large areas above the Mediterranean Sea in all air mass types. Maximum concentrations of particles in the size range 5 – 10 nm ( $N_{5-10}$ ) do not systematically coincide with lower fetches (time spent by the air mass over the sea before sampling), and significant  $N_{5-10}$  values are found for fetches between 0 and 60 hours depending on the air mass type. These observations suggest that nucleation events could be more influenced by local precursors originating from emission processes occurring above the sea, rather than linked to synoptic history. Vertical soundings were performed, giving the opportunity to examine profiles of the  $N_{5-10}$  concentration and to analyse the vertical extent of NPF. Our observations demonstrate that the process could be favoured above 1000 m, i.e. frequently in the free troposphere, and more especially between 2000 and 3000 m, where the NPF frequency is close to 50 %. This vertical

1 distribution of NPF might be favoured by the gradients of several atmospheric parameters,  
2 together with the mixing of two air parcels which could also explain the occurrence of the  
3 process at preferential altitudes. In addition, increased condensation sinks collocated with  
4 high concentrations of small particles suggest the occurrence of NPF events promoted by  
5 inputs from the boundary layer, most probably associated with convective clouds and their  
6 outflow. After they formed, particles slowly grow at higher altitudes to diameters of at least  
7 30 nm while being poorly depleted by coagulation processes. Our analysis of the particle size  
8 distributions suggests that particle growth could decrease with increasing altitudes.

9

## 10 **1 Introduction**

11 New particle formation (NPF) is a widespread phenomenon in the atmosphere which results  
12 from a complex sequence of multiple processes including two major steps (Kulmala and  
13 Kerminen, 2008): 1) the formation of clusters from the gaseous phase and 2) the growth of  
14 these clusters up to sizes at which they may influence the climate through cloud related  
15 radiative processes (Kerminen et al., 2012; Makkonen et al., 2012). Observations of the  
16 phenomenon in various environments are reported in the literature (Kulmala et al., 2004),  
17 including boundary layer (BL) polluted locations (e.g. Brock et al., 2003; Wiedensohler et al.,  
18 2009), clean or rural sites (e.g. Suni et al., 2008), high altitude stations (e.g. Venzac et al.,  
19 2008; Boulon et al., 2010; Rose et al., 2014), polar areas (e.g. Asmi et al., 2010), and coastal  
20 sites (e.g. O'Dowd et al., 1998; 2002). NPF events characteristics, such as spatial extent, both  
21 vertical and horizontal (Crumeyroille et al., 2010; Boulon et al., 2011), particle formation and  
22 growth rates (Manninen et al., 2010; Yli-Juuti et al., 2011) are known to be affected by  
23 atmospheric parameters, including the amount of gaseous precursors, the concentration of  
24 pre-existing aerosol particles and meteorological variables (temperature, relative humidity,  
25 solar radiation). However, current knowledge of the theory that lays beyond NPF remains  
26 poor, especially at high altitudes, ie above 1000 m, and a more profound understanding of the  
27 mechanisms and precursors involved in nucleation and particle growth is currently required,  
28 especially to improve the accuracy of climate modelling studies.

29 Marine aerosol particles, as one of the main contributors to the natural aerosol emissions, has  
30 focussed the attention of the scientific community for several decades (eg: Heintzenberg et al.,  
31 2000 and references therein). In these pristine environments, changes in the aerosol burden  
32 might have significant impacts on cloud properties, as shown in recent studies (Tao et al.,

1 2012; Koren et al., 2014; Rosenfeld et al., 2014). Marine aerosol has a primary component,  
2 known as “sea spray aerosol”, which results from the interaction between wind and water  
3 surface, and a secondary component, which is in the scope of the present work. Current  
4 knowledge regarding NPF in the marine boundary layer mainly concerns coastal regions  
5 (O’Dowd et al., 1998; 2002; 2007), where observations of NPF are more abundant than over  
6 the open ocean. Many studies have concentrated on the comprehension of the mechanisms  
7 and the identification of the precursors involved in the NPF process from coastal magroalga  
8 fields (O’Dowd and Leeuw, 2007 and references therein), including both model studies  
9 (Pirjola et al., 2000) and chamber experiments (Sellegrri et al., 2005). A schematic view of the  
10 marine aerosol production in coastal areas based on observations from the Mace Head station  
11 (Ireland) is given by Vaattovaara et al. (2006). In contrast, the scarcity of open ocean  
12 nucleation studies reported in the literature might indicate that the NPF process does not occur  
13 with a high probability over open ocean.

14 While ground based stations allow indirect analysis of the horizontal extent of NPF  
15 (Kristensson et al., 2014; Rose et al., 2015), airborne aerosol measurements can add relevant  
16 information both on the horizontal and on the vertical extent of NPF. Such measurements  
17 were conducted over the boreal environment, in the vicinity of the Hyytiälä SMEAR-II  
18 station, using aircrafts (O’Dowd et al., 2009; Schobesberger et al., 2013) but also motorized  
19 hang glider/microlight aircraft (Junkermann, 2001; 2005) or balloons (Boy et al., 2004;  
20 Laakso et al., 2007). These studies, based on a limited number of observations, delivered  
21 contrasting results indicating that nucleation could occur throughout the boundary layer, but  
22 also in the free troposphere in some cases (Laakso et al., 2007), with no clear trend or  
23 preference. Airborne studies conducted in different environments are also reported in the  
24 literature, showing evidence for the occurrence of NPF in the free troposphere above Europe  
25 during the EUCAARI-LONGREX project (Mirme et al., 2010) and above the Arctic region,  
26 up to 7 km, by Khosrawi et al. (2010) during the project ASTAR 2004. In contrast, using a  
27 restricted number of aircraft vertical soundings, Crumeyrolle et al. (2010) suggest that over  
28 the North Sea, NPF could be limited to the top of the boundary layer.

29 Giving more insights in the vertical development of the NPF process in the marine  
30 troposphere is one of the main objectives of the present study based on aircraft measurements  
31 conducted above the Mediterranean sea between the 11<sup>th</sup> of September and the 4<sup>th</sup> of  
32 November 2012 in the framework of the HYMEX (HYdrological cycle in Mediterranean

1 EXperiment) project. We report particle size distributions and concentrations measured with a  
2 Scanning Mobility Particle Sizer (SMPS) and Condensation Particle Counters (CPC)  
3 deployed on board the French ATR-42 aircraft. The occurrence of NPF is investigated, with a  
4 special focus on the horizontal and vertical extents of the process, coupled with an analysis of  
5 several atmospheric parameters expected to explain these extents.

## 6 **2 Measurements and methods**

### 7 **2.1 Instruments on board ATR-42 aircraft**

8 As part of the HYMEX project, the ATR-42 research aircraft operated by SAFIRE (Service  
9 des Avions Français Instrumentés pour la Recherche en Environnement) was based at  
10 Montpellier airport, in the south of France. A total of 28 flights were performed between the  
11 11<sup>th</sup> of September and 4<sup>th</sup> of November 2012 (Table 1).

12 The instrumental setup deployed on board and used for the analysis of NPF consisted of two  
13 Condensational Particle Counters (CPC) and a Scanning Mobility Particle Sizer (SMPS). The  
14 CPCs, developed at the Max Planck Institute for Polymer Research, Mainz, Germany, are  
15 specifically dedicated to aircraft measurements (Weigel et al., 2009). Their nominal 50%  
16 lower cut-off diameter can be varied by changing the temperature difference between  
17 saturator and condenser. During HYMEX, one of the CPCs was measuring with a cut-off  
18 diameter of 5 nm and the second with a cut-off diameter of 10 nm. The time resolution of the  
19 CPCs was set to 1 second. The SMPS system was previously described in Crumeyrolle et al.  
20 (2010) and consists of a CPC (TSI, 3010), a Differential Mobility Analyzer (DMA) and a  
21 krypton aerosol neutralizer. The SMPS provided particle size distributions in the diameter  
22 range 20 – 485 nm, with a time resolution of 130 seconds.

23 The ATR-42 was also equipped with additional instruments dedicated to the analysis of  
24 aerosol and cloud properties: Particle Soot Absorption Photometer allowing the monitoring of  
25 black carbon concentration (PSAP, Bond et al., 1999), Optical Particle Counter (OPC,  
26 GRIMM), a compact Aerosol time of flight Mass Spectrometer (AMS, Drewnick et al., 2005)  
27 and Fast Forward Scattering Spectrometer Probe (Fast-FSSP). The aerosol instrumentation  
28 was connected to the community aerosol inlet (CAI) which has a 50% sampling efficiency for  
29 particles larger than 5  $\mu\text{m}$  (see Crumeyrolle et al., 2010 and references therein for more  
30 details). Routine meteorological variables were continuously monitored.

## 1 2.2 Data analysis

### 2 2.2.1 Sea/land mask

3 The main objective of this study was to investigate the occurrence of NPF in the marine  
4 troposphere. For that purpose, all measurements conducted above land were removed from  
5 the database. An arbitrary threshold distance of 1 km to the coast was set to consider  
6 measurement as “marine”. The distance  $D$  between two geographical points  $A$  and  $B$ ,  
7 knowing their coordinates, was calculated according to:

$$8 \quad D = \arccos(\sin(\varphi_A) \times \sin(\varphi_B) + \cos(\varphi_A) \times \cos(\varphi_B) \times \cos(\lambda_A - \lambda_B)) \times R_T \quad (1)$$

9 Where  $\varphi_Y$  and  $\lambda_Y$  are the latitude and longitude of the location  $Y$ , respectively, and  $R_T =$   
10 6371 km is the mean radius of the Earth. The position of the points located at the threshold  
11 distance of  $1000 \pm 50$  m from the aircraft position was calculated using Eq. (1) every 10  
12 seconds along the flight path (which correspond to a distance of 1 km for a typical aircraft  
13 speed of  $100 \text{ m s}^{-1}$ ) and plotted on a map. Measurements were considered as “marine” when  
14 none of these points (forming an ellipse) intercepted any coastline, as illustrated on Fig. 1.  
15 We finally assumed that the flag (“marine” or “land”) obtained at a time  $t$  was the same for  
16 the 5 seconds that preceded  $t$  and the 4 seconds that followed  $t$ .

### 17 2.2.2 Detection of nucleation events

18 In order to track the occurrence of nucleation above the Mediterranean Sea and to evaluate the  
19 strength of the events, particle concentration in the size range 5 – 10 nm ( $N_{5-10}$ ) was  
20 calculated by subtracting the data readings of the two CPCs. After analysing the variability of  
21  $N_{5-10}$  apart from nucleation periods, we found that  $N_{5-10}$  concentrations had an average value  
22 of  $29.9 \text{ cm}^{-3}$  and a standard deviation of  $144.8 \text{ cm}^{-3}$ . Hence,  $N_{5-10}$  concentrations were  
23 considered significant above the threshold value of  $175 \text{ cm}^{-3}$ . It is worth noticing that in-cloud  
24 measurements were filtered out in order to prevent the detection of elevated particle  
25 concentrations that could be sampling artefacts linked to the fragmentation of cloud droplets  
26 impacting the aerosol inlet (Weber et al., 1998).

### 27 2.2.3 Air mass back trajectories

28 The influence of air mass history on the occurrence of nucleation was studied using three days  
29 air mass back trajectories computed with the HYSPLIT transport and dispersion model

1 (Draxler and Rolph, 2003). Three days before sampling were chosen based on previous work  
2 by Tunved et al. (2005) who estimated the turnover time of aerosol particles to be around 1.6-  
3 1.7 days for nuclei size ranges and 2.4 days for 200 nm particles. Back trajectories were  
4 calculated every 5 minutes along the flight path (i.e. 30 km for a typical aircraft speed of 100  
5 m.s<sup>-1</sup>) and air masses were further classified into Northern Europe, Western Europe, Southern  
6 Mediterranean Sea, Eastern Mediterranean Sea and Local types according to the maximum  
7 time spent in each sector. As illustrated on Fig. 2, the Local sector corresponds to the  
8 geographical area where most of the flights took place during the HYMEX campaign (centred  
9 on the position 41.6701°/6.8769°), while Northern Europe, Western Europe, Southern  
10 Mediterranean Sea and Eastern Mediterranean Sea types are related to the sectors 45 – 135°,  
11 135 – 225°, 225 – 315° and 315 – 45°, respectively. We made the assumption that the air  
12 mass origin obtained at a time  $t$  was the same for the 150 seconds that preceded  $t$  and the  
13 149 seconds that followed  $t$ .

### 14 **3 Results and discussion**

#### 15 **3.1 Observation of nucleation events above the Mediterranean Sea**

##### 16 **3.1.1 Horizontal extent**

17 When considering all measurements recorded in clear sky conditions above the sea, 26% of  
18 N<sub>5-10</sub> concentrations were found to exceed the threshold value. These concentrations are  
19 obtained at all times, with slightly increased probabilities in the afternoon (11:00 – 17:00  
20 UTC, 29%) compared to other time periods (23% for 05:00 – 11:00 UTC and 24% for 17:00 –  
21 05:00 UTC). The fact that night time could be associated to similar probabilities for the  
22 detection of significant N<sub>5-10</sub> values compared to morning hours was quite unexpected since  
23 nucleation events are more frequently reported to be initiated in the morning (e.g. Dal Maso et  
24 al., 2005; Rose et al., 2015). In fact, night time events have already been observed, but appear  
25 to be more scarce (Lee et al., 2008; Suni et al., 2008). The origin of nanoparticles observed at  
26 night in the present study is further discussed in Section 3.2.2.

27 The location where the significant N<sub>5-10</sub> concentrations (> 175 cm<sup>-3</sup>) were detected is shown  
28 on Fig. 3. The map we obtain clearly indicates that nanoparticle concentrations are detected  
29 above the sea over large areas, being continuously detected along the flight paths over  
30 distances that can reach ~580 km (flight 52). N<sub>5-10</sub> concentrations are in the range 235 (25<sup>th</sup>  
31 perc.) – 563 (75<sup>th</sup> perc.) cm<sup>-3</sup>, with a median value of 328 cm<sup>-3</sup>. This range is of the order of

1 magnitude of concentrations measured by the SMPS for larger particles (Table A1) above  
2 2000 m, which indicates that nucleated particles may contribute significantly to the total  
3 aerosol burden after they have grown.

4 According to the geographical distribution of the nucleation points in Fig. 3, it is likely that  
5 nucleation could occur at variable distances to the coast. Small particles observed close to the  
6 littoral may be expected to be produced during events initiated above land or involving  
7 gaseous precursors originating from the continental boundary layer (BL). In contrast,  
8 significant  $N_{5-10}$  concentrations measured hundreds of kilometres far from the shore suggest  
9 the occurrence of events which are more disconnected from continental sources, and could be  
10 rather associated with marine precursors. This point is further discussed in the following  
11 section.

### 12 3.1.2 Influence of air mass origin – fetch of air masses

13 As reported in Table 1, most of the studied flights were performed under Western Europe and  
14 Southern Mediterranean Sea atmospheric flows (15 and 7 out of 28, respectively), while  
15 northern and local types were only observed during three flights. The three remaining flights  
16 were performed under variable conditions, however often dominated by Western Europe and  
17 Southern Mediterranean Sea flows.

18 Significant concentrations of small particles in the size range 5 – 10 nm were detected in all  
19 types of air masses (Table 2), but the highest nucleation probability was found in northern air  
20 masses, where 60% of  $N_{5-10}$  values exceeded the threshold value. In contrast, Eastern  
21 Mediterranean Sea flows showed the lowest nucleation probability, of around 0.4%.  
22 However, the values obtained for eastern, northern and local air masses may not be relevant as  
23 we have very little statistics on them. For this reason, eastern, northern and local flows will  
24 not be further discussed. In Western Europe and South Mediterranean Sea air masses, the  $N_{5-10}$   
25 threshold value was exceeded in 23 and 32% of the cases studied, respectively. It is worth  
26 noticing that the frequency of occurrence of significant ultrafine particle concentrations is  
27 relatively important in southern air masses, i.e. in air masses that have spent a significant time  
28 over the Mediterranean Sea, free of the influence of recent continental emissions.

29 Median  $N_{5-10}$  concentrations calculated for western and southern flows were on average very  
30 similar, 315 and 361  $\text{cm}^{-3}$ , respectively. Based on the interquartile range (IQR), the variability  
31 of  $N_{5-10}$  concentrations was relatively low for these two air mass types (IQR = 336 and 323

1  $\text{cm}^{-3}$ , respectively). These results suggest that the strength of the events and the number of  
2 nucleated particles are not deeply impacted by air mass origin, and could instead be  
3 influenced by local (marine) atmospheric conditions.

4 In order to further investigate this aspect, a more detailed analysis of the number of nucleated  
5 particles as a function of the fetch, i.e. the time spent by air masses above the sea before  
6 sampling, was conducted and is reported on Fig. 4, separately for Western Europe and South  
7 Mediterranean Sea flows. Reported  $N_{5-10}$  are averaged concentrations calculated from the 60  
8 second periods spanning around the times used for air mass back trajectories computation.

9 In Western Europe and South Mediterranean Sea air masses, fetches up to 60 hours were  
10 calculated. In these air masses, larger concentrations are typically recorded for smaller  
11 fetches, with maximum  $N_{5-10}$  values obtained for fetches around 5 hours. This last observation  
12 could either indicate that events are influenced by precursors from marine origin and have a  
13 growth rate higher than  $0,8 \text{ nm h}^{-1}$ , or that the detected clusters were produced over the  
14 continent and need 4 to 5 hours before being detected by our CPC tandem. However, we do  
15 detect significant concentrations of particles in the 5-10 nm size range in air masses with  
16 fetches up to 60 hours, which clearly suggests a significant marine contribution for these  
17 events and would indicate that the Mediterranean troposphere houses precursors of  
18 nucleation.

19 The purpose of the next section is now to investigate the vertical extent of nucleation.

### 20 3.1.3 Vertical extent

21 A total of 39 vertical soundings were performed during the studied flights, giving the  
22 opportunity to examine profiles of the  $N_{5-10}$  particle concentrations. Such profiles are shown  
23 in Fig. 5. Boundary layer height (BLH) is also provided as additional information for each  
24 sounding. BLH was obtained using interpolation in space and time from the diagnosed BLH  
25 retrieved by the European Centre for Medium Range Weather Forecasts (ECMWF) at forecast  
26 times of 3, 6, 9, 12, 15, 18, 21 and 24 hours, starting at 00:00 UTC, and horizontal resolution  
27  $0.25^\circ$ . Estimations of the BLH were also obtained from the analysis of the vertical gradients  
28 of temperature, potential temperature, relative humidity and specific humidity, as suggested  
29 by Seidel et al. (2010). Reasonable agreement was found between the “gradient method” and  
30 ECMWF BLHs.



1 For most of the soundings, the BLH was lower than 1000 m, being on average  $662\pm 325$  m.  
2 Fifteen profiles shown on Fig. 5 are not sufficient to allow a complete vertical investigation of  
3 both boundary layer (BL) and free troposphere (FT) altitudes and were thus left out (profiles  
4 n°1, 7, 10, 11, 14, 15, 16, 20, 21, 22, 23, 24, 25, 37 and 39). For 17 of the 24 remaining  
5 profiles,  $N_{5-10}$  concentrations exceeding the threshold value are mainly found above the BL,  
6 indicating that nucleation could most probably occur in the FT (profiles n°2, 6, 13, 17, 18,  
7 19, 26, 27, 29, 30, 31, 32, 33, 34, 35, 36 and 38). Only 3 profiles (n°3, 4, 5), obtained during  
8 take-off/landing phases, show the opposite, with significant  $N_{5-10}$  constrained to BL altitudes.  
9 Small particles are observed both in the BL and in the FT with no preferential altitudes  
10 identified during one sounding (28), and three profiles do not show any indication of  
11 nucleation (n°8, 9 and 12).

12 The vertical limits of the nucleation process are clearly visible for profiles n°6 and 27. For  
13 profile n°6, nucleation is observed between 1680 and 3170 m, with concentrations  
14 significantly increased between 2400 and 2900 m. During sounding n°27, nucleation is  
15 detected on a slightly more restricted altitude range, 1350 – 1780 m, with higher  
16 concentrations between 1660 and 1710 m. Other profiles, such as n°18, 23 and 34, also  
17 display  $N_{5-10}$  values which are significantly increased on a well defined atmospheric layer  
18 above 1000 m, not only indicating that nucleation could be promoted at higher altitudes, but  
19 also suggesting the existence of preferential altitudes.

20 In order to further investigate the vertical extension of nucleation, all measurements were  
21 considered, i.e.  $N_{5-10}$  concentrations measured during vertical soundings and also at constant  
22 altitude levels. Fig. 6 (left panel) shows the percentage of  $N_{5-10}$  concentrations exceeding the  
23 threshold value as a function of altitude range. As previously suggested by Fig. 5, nucleation  
24 seems to be favoured above 1000 m. In fact, below 1000 m, less than 4% of the recorded  
25 concentrations were found to be significant. In contrast, nucleation probability is increased by  
26 10 above 1000 m, and it is worth noticing that almost 50% of the concentrations obtained  
27 between 2000 and 3000 m exceed the threshold value, indicating that these altitudes could  
28 more especially favour the occurrence of nucleation.

29 However, it seems that when nucleation events are detected, the number of nucleated particles  
30 does not significantly vary with altitude, especially above 500 m, where median  
31 concentrations are in the range  $307 - 376 \text{ cm}^{-3}$  (Fig. 6, right panel). Below 500 m,  $N_{5-10}$  are

1 slightly increased and show higher variability, which might be caused by more  
2 inhomogeneous conditions found in this part of the atmosphere compared to higher altitudes.

3 The fact that nucleation could be favoured in the FT compared to the BL contradicts the  
4 results by Crumeyrolle et al. (2010), who found that NPF events were limited to the top of the  
5 BL in the North Sea. However it is worth noticing that the number of vertical profiles  
6 included in the Crumeyrolles study was limited (13 profiles), and most of them were  
7 performed close to the coast.

#### 8 3.1.4 Why such a vertical extension?

9 The purpose of this section is to further investigate atmospheric parameters and/or processes  
10 which are associated to the higher probability of observation of small particles at higher  
11 altitudes.

12 Meteorological parameters, such as temperature and relative humidity (RH), as well as global  
13 radiation, were previously reported to influence the nucleation process. Global radiation,  
14 which is expected to be more intense at higher altitudes, and thus favor photochemical  
15 processes, including the oxidation of gaseous precursors involved in the nucleation process,  
16 could give a first explanation to the observed  $N_{5-10}$  vertical distribution. While low  
17 temperatures were also found to favor nucleation (Young et al., 2007), the role of RH seems  
18 to be more ambiguous. In fact, nucleation is likely to occur preferentially at low RH (Birmili  
19 et al., 2003), and both the nucleation rate and nucleated cluster concentration are reported to  
20 be anti-correlated with RH (Jeong et al., 2004; Sihto et al., 2006). However, nucleation events  
21 have been detected in the vicinity of clouds, where high RH are found (Clarke et al., 1998).  
22 Another aspect to consider is that among high altitude air masses, increased RH would also be  
23 associated to intrusions from the BL and hence more gaseous precursors and higher CS. The  
24 possibility for the small particles that were detected at high altitude to originate from NPF  
25 events associated with convective clouds and their outflow will be further investigated in the  
26 following.

27 Statistics concerning temperature and RH recorded during the studied flights are presented as  
28 a function of altitude range on Fig. 7. It is very clear that temperature is decreasing with  
29 altitude, especially above 3000 m where most of the temperatures are found to be below zero.  
30 The same trend is observed for RH, but with higher variability.  $N_{5-10}$  concentrations were also  
31 directly considered as a function of temperature, RH and humidity mixing ratio ( $\text{g kg}^{-1}$ ), but

1 the correlations between these meteorological parameters and the particle concentration was  
2 weak at all altitudes ( $|R^2| < 0.2$ ).

3 Figure 8 shows, for the different altitude ranges previously introduced, the median  
4 condensation sink (CS) calculated from SMPS size distributions recorded at constant  
5 altitudes, i.e. apart from vertical soundings. Up to 2000 m, the median CS does not  
6 significantly vary with altitude, being in the range  $3.1 - 3.9 \times 10^{-3} \text{ s}^{-1}$ . A higher variability  
7 observed below 500 m could again be explained by more inhomogeneous conditions found at  
8 low altitudes. Above 2000 m, CS values are significantly decreased, with median values  
9 below  $10^{-3} \text{ s}^{-1}$ . These first observations suggest that higher nucleation frequencies found  
10 above 2000 m could be, at least partly, explained by lower CS. The fact that nucleation could  
11 be promoted at higher altitudes due to lower CS values was also reported by Boulon et al.  
12 (2011) at the puy de Dôme (PUY) station (1465 m a.s.l, France), where NPF is observed  
13 twice as frequently as at the BL station of Opme (660 m a.s.l.) located 12 km south east of the  
14 PUY.

15 A more complete analysis focussed on altitudes above 2000 m was then conducted to  
16 highlight the role of the CS in the nucleation process at higher altitudes. Figure 9 shows the  
17 correlation between  $N_{5-10}$  particle concentration and CS, separately for the two altitude ranges  
18 above 2000 m. The  $N_{5-10}$  shown are 130 second averaged values coinciding with SMPS  
19 measurements used for the CS calculation. Based on Fig. 8, we observe that ultrafine particle  
20 concentration and CS are positively correlated within each altitude range, especially between  
21 2000 and 3000 m ( $R^2 = 0.48$ ). The lack of measurements did not allow similar analysis at  
22 lower altitudes to compare with, but the fact that at higher altitudes, where the CS is usually  
23 low compared to BL stations, increased CS could favour the occurrence of nucleation has  
24 already been reported in the literature (Boulon et al., 2010; Rose et al., 2014). While lower CS  
25 values are typically reported on event days compared to non-event days at BL sites, increased  
26 CS are found on event days at high altitude stations (Manninen et al., 2010).

27 In the present study, we may hypothesize that some gaseous compounds are transported,  
28 together with the pre-existing particles, from lower altitudes, and that they may be further  
29 oxidized to more condensable species involved in the nucleation process. As previously  
30 mentioned, such processes might be favoured by convection associated with clouds and their  
31 outflow. In that case, the lifted air parcels where small particles are detected are expected to  
32 have different chemical signature from free troposphere air, as well as different water vapour

1 content. Also, the fact that clusters might be formed at lower altitudes and then be transported  
2 together with larger particles above 2000 m cannot be excluded. In addition, it has been  
3 previously reported by several studies that the mixing of two air parcels showing contrasting  
4 levels of RH, temperature, condensation sink and precursors, could favor the occurrence of  
5 nucleation (Nilsson and Kulmala, 1998; Khosrawi and Konopka, 2003; Dall'Osto et al.,  
6 2013).

7 We further investigated the contribution of cloud processes and BL intrusions regarding the  
8 formation of new particles using tracers such as the black carbon (BC) concentration and the  
9 specific humidity, in addition to cloud cover. Unfortunately, there was no measurement  
10 available regarding the composition of the gas phase. Our analysis was focussed on the  
11 vertical soundings performed by the ATR-42 that allow a direct comparison of the vertical  
12 distribution of the parameters of interest (Fig. 5 and S1).

13 Among the 17 profiles previously associated to NPF in the FT (profiles n°2, 6, 13, 17, 18, 19,  
14 26, 27, 29, 30, 31, 32, 33, 34, 35, 36 and 38), although cloudy conditions were filtered from  
15 our analysis, we retrieved that clouds were observed in the same altitude range as small  
16 particles in 4 cases (profiles n° 29, 30, 34 and 38). For 3 of them, collocated increases of the  
17 specific humidity (profiles n° 29 and 30) and/or BC concentration (profiles n° 30 and 34)  
18 were also found. These observations suggest that for those 4 particular cases, the formation of  
19 small particles was most probably induced in recently lifted air from convective clouds. For  
20 the remaining soundings, clouds were detected at lower altitudes: for soundings n° 2, 6, 13,  
21 18, 19, 31, 33, 35 and 36, the vertical cloud profile was sparse, while it was denser for profiles  
22 n° 17, 26, 27 and 32. Missing data did not allow a complete analysis of soundings n° 18 and  
23 36, which will thus not be further discussed. During sounding n°31, high  $N_{5-10}$  were found in  
24 the close vicinity of the cloud. The origin of small particles observed during profiles n° 6, 13,  
25 27 and 32 could not be stated unambiguously, since they were observed at altitudes  
26 characterized by low BC concentrations but median specific humidity. In contrast, the vertical  
27 distributions associated to profiles n° 2, 17, 26, 33 and 35 clearly suggest the occurrence of  
28 NPF events in free tropospheric conditions, free of the influence of recent BL inputs. In  
29 addition, during sounding n° 19, small particles were detected around 1000 m and slightly  
30 below 4000 m, while increased specific humidity and BC concentrations were observed  
31 between 2000 and 2500 m.

1 We have shown so far that above the Mediterranean Sea, NPF was observed over large areas  
2 and could be favoured at higher altitudes, since particles in the size range 5-10 nm are mostly  
3 seen above 1000 m. However, the previous analysis did not always unambiguously answer  
4 the question regarding the conditions associated to the initial cluster (1-2 nm particles)  
5 formation, especially in terms of the degree of BL influence/intrusions. Nonetheless, these  
6 particles, whatever transported to or formed in the FT, in more or less polluted conditions, are  
7 expected to grow to larger diameters and might reach climate relevant sizes in the FT. The  
8 purpose of the next section is to investigate this growth process above 2000 m by analysing  
9 the shape of the SMPS size distributions.

## 10 **3.2 Investigation of particle growth above 2000 m**

### 11 **3.2.1 Analysis of SMPS particle size distributions**

12 All SMPS size distributions (20.4 - 484.5 nm) recorded at constant altitude were fitted with  
13 four Gaussian modes: a nucleation mode with a mean diameter around 25 nm, an Aitken  
14 mode with a mean diameter around 50 nm, a first accumulation mode with a mean diameter  
15 around 110 nm and a second accumulation mode centred around 220 nm as initial guesses.  
16 These four modes were chosen because they most frequently came out of the fitting procedure  
17 when run without initial guesses. These diameters were previously found in the literature to  
18 describe particle size distributions in the marine atmosphere (Heintzenberg et al., 2000). The  
19 geometric mean diameters of these modes found by the fitting procedure vary from the initial  
20 guesses with time and altitude. In the following sections, the parameters of the modes  
21 (geometric mean diameter and concentration) will be used to describe the evolution of the  
22 particle size distribution.

23 Figure 10 shows the average fitted distributions as a function of altitude and daytime. The  
24 analysis is focussed on the highest altitude ranges, where nucleation was more frequently  
25 observed (the altitude range 1000 – 2000 m is not considered because of a too small number  
26 of data points). The parameters of the Gaussians used for these fits are given as additional  
27 information in Table A1. The “closed” shape of the reconstructed size distributions shown on  
28 Fig. 10 is the result of the originally “open” type size distributions that were fitted with a  
29 nucleation mode that extended below the SMPS lower size cut (20 nm). These reconstructed  
30 size distributions do represent the real size distributions measured below 20 nm.

1 During the time period 11:00 – 17:00 UTC, the size distributions are dominated by the  
2 nucleation mode. In fact, this mode includes 42% of the particles measured by the SMPS  
3 between 2000 and 3000 m, and 48% above 3000 m. However, both the concentration and the  
4 diameter of the nucleation mode appear to be larger between 2000 and 3000 m compared to  
5 higher altitudes (Table A1). Since  $N_{5-10}$  concentrations were shown to be comparable for the  
6 two altitude ranges (Fig. 7), a faster growth at lower altitudes supported by a larger pool of  
7 condensable species could explain the differences observed on the size distributions.

8 At night (17:00 – 05:00 UTC), the contributions of nucleation and Aitken modes to the total  
9 particle concentration are very similar between 2000 and 3000 m, being around 34% each,  
10 whereas above 3000 m the nucleation mode is dominant (46% against 36% for the Aitken  
11 mode). These observations suggest that between 2000 and 3000 m, nucleated particles are  
12 growing during the course of the day, leaving the nucleation mode, which thus includes a  
13 decreasing fraction of the total particle concentration, to reach the Aitken mode. In contrast, it  
14 is likely that above 3000 m, particle growth is not as fast, since the nucleation mode displays  
15 particle concentrations which remain on average higher compared to the Aitken mode, even in  
16 the evening. Again, this observation suggests that particle growth could get slower with  
17 increasing altitudes.

18 In the morning (05:00 – 11:00 UTC), the average size distribution above 3000 m displays a  
19 nucleation mode which diameter is similar to the diameter observed at night (~ 23 nm), and  
20 with a contribution to the total particle concentration which is significantly higher than the  
21 contribution of the Aitken mode (62 and 21%, respectively). In contrast, between 2000 and  
22 3000 m, the nucleation mode displays a large diameter (30.5 nm) and a contribution which is  
23 lower than the contribution of the Aitken mode (30 and 51%, respectively). We may  
24 hypothesize that the small particles which are seen in the nucleation mode above 3000 m do  
25 not originate from nucleation events initiated in the morning, but were rather formed the day  
26 before and are still undergoing a very slow growth process. The low concentration of  
27 nucleation mode particles between 2000 and 3000 m might be explained by a faster growth  
28 for the particles formed the day before, which have thus reached larger diameters, and also by  
29 the fact that particles nucleated in the morning (the nucleation probability between 2000 and  
30 3000 m during the time period 05:00 - 11:00 UTC is 23%) may not have already reached the  
31 lower detection limit of the SMPS.

### 1 3.2.2 Origin of night time nanoparticles

2 As previously mentioned, nanoparticles in the size range 5 – 10 nm were detected during  
3 night time (17:00 – 05:00 UTC). The purpose of this last section is to investigate their origin,  
4 and more particularly to examine the possibility for the night time particles to originate from  
5 nucleation events triggered earlier during day time.

6 The time interval 09:00 – 12:00 UTC, during which the formation of cluster particles is most  
7 frequently observed (Rose et al., 2014; 2015), was considered as a reference nucleation  
8 period, and only the significant 130 second averaged  $N_{5-10}$  concentrations obtained between  
9 09:00 and 12:00 UTC were further considered. We estimated the half-life time of these  
10 particles, i.e. the time  $t_{fin}$  at which these concentrations reached half of their initial values,  
11 obtained at  $t_0$ , under the following assumptions: 1) particles are removed from the size range 5  
12 – 10 nm by coagulation and growth processes and 2) the coagulation sink calculated at  $t_0$  is  
13 constant during particle growth.  $t_{fin}$  is finally given by Eq. (2):

$$14 \quad t_{fin} = t_0 + \frac{0.5}{Coag + \frac{f}{5} * GR} \quad (2)$$

15 Where Coag is the coagulation sink of 5 nm particles derived from SMPS data, and GR is the  
16 particle growth rate. The factor f represents the fraction of the aerosol population which is  
17 activated for growth, and was assumed to be equal to unity.

18 Particle GR were estimated from the shift of the nucleation mode diameter observed on the  
19 average SMPS size distributions between night time (17:00 – 05:00 UTC) and morning hours  
20 (05:00 – 11:00 UTC) for the altitude range 2000 – 3000 m (Table A1, Fig. 10). An average  
21 value of 0.31 nm h<sup>-1</sup> was found. However, GR was previously reported to increase with  
22 particle size (Yli-Juuti et al., 2011; Kulmala et al., 2013), this is the reason why lower GR of  
23 0.1 nm h<sup>-1</sup> was also used to describe particle growth in the size range 5 – 10 nm. In order to  
24 complete our sensitivity study regarding the GR, additional higher value of 1 nm h<sup>-1</sup> was  
25 selected. The results of this analysis are reported on Fig. 11, which indicates that particle life  
26 time increases with altitude. Such observation might be explained by decreasing total particle  
27 concentrations with increasing altitude, thus leading to lower coagulation sinks. Considering  
28 the scenario with intermediate GR of 0.3 nm h<sup>-1</sup>, initial  $N_{5-10}$  concentrations are all divided by  
29 two before night time, suggesting that, considering the relatively high concentrations found at  
30 night, there would be an additional source of 5-10 nm particles above 2000 m. The same

1 conclusion is obtained with  $GR = 1 \text{ nm h}^{-1}$ . In contrast, using the more probable value of  $GR$   
2  $= 0.1 \text{ nm h}^{-1}$ , we observe that for some cases, nanoparticle concentration reach half of its  
3 initial value only after 17:00 UTC, or even later. Because of the reduced number of data  
4 points, these conclusions must be considered with caution but it is likely that a large fraction  
5 of nanoparticles detected during the night could be formed earlier during the day. The  
6 subsistence of the nanoparticles in the size range 5 – 10 nm might be explained by low  
7 coagulation sinks coupled with slow particle growth.

#### 8 **4 Conclusion**

9 We investigated the occurrence of nucleation events above the Mediterranean Sea using data  
10 obtained during research flights performed in the framework of the HYMEX project between  
11 September and November 2012.

12 Based on our observations, nucleation takes place over large areas above the Mediterranean  
13 Sea in all air mass types. Nucleation probability slightly varies with air mass origin, but the  
14 signature of the different air mass types is however complex to distinguish in terms of  $N_{5-10}$   
15 concentrations. In Western Europe and South Mediterranean Sea flows, more frequently  
16 observed compared to other air mass types, maximum concentrations were obtained for  
17 fetches around 5 hours, but significant concentrations persist over fetches up to 60 hours,  
18 suggesting that the nucleation process could be more influenced by parameters inherent of the  
19 marine troposphere.

20 The analysis of the vertical extension of nucleation showed that the process could be  
21 promoted above 1000 m, and especially between 2000 and 3000 m. Simultaneous analysis of  
22 the boundary layer height indicated that these altitudes often corresponded to free  
23 tropospheric conditions. Vertical gradient of the condensation sink, together with temperature  
24 and humidity might explain the increasing nucleation probability with altitude. The mixing of  
25 two air parcels with contrasting properties (temperature, RH, condensation sink, precursors)  
26 could also support the occurrence of nucleation at preferential altitudes. In addition, for a  
27 given altitude range, larger  $N_{5-10}$  concentrations were often co-located with increased CS,  
28 likely associated with higher oxidation of gas phase precursors. This last observation suggests  
29 inputs from the BL that might be the result of convective movements of air parcels induced by  
30 clouds and their outflow. The fact that clusters might also be transported from lower altitudes  
31 through such processes cannot be excluded.



1 The investigation of the global shape of the particle size distributions derived from SMPS  
 2 measurements finally allowed us to study the particle growth above 2000 m, and more  
 3 particularly the relative contribution of the different particle modes to the total concentration  
 4 as a function of time and altitude. After they formed, particles appear to grow to larger sizes  
 5 above 2000 m, reaching the Aitken mode range, but with growth rates which seem to decrease  
 6 with altitude. This slow growth, coupled with low coagulation sinks, may favour longer  
 7 subsistence for nanoparticles in the size range 5 – 10 nm, and could explain the detection of  
 8 these small particles during night time, several hours after their formation.

9 Our findings demonstrate that higher altitudes could promote the occurrence of NPF, not only  
 10 over continental areas, as previously suggested by Boulon et al. (2011), but also over open  
 11 seas, with indications of marine precursors. This result supports the model study by  
 12 Makkonen et al. (2012), which predicts that nucleation could have a significant contribution  
 13 to the cloud condensation nuclei (CCN) concentration over the Mediterranean Sea, and  
 14 indicates that this contribution could be even more decisive at higher altitudes, where clouds  
 15 form.

## 16 **Appendix A**

17 Table A1. Parameters of the Gaussians used to fit the SMPS size distributions as a function of  
 18 daytime for the altitude ranges above 2000 m.

19 a) 05:00 – 11:00

Mode	Parameters	2000 – 3000 m	>3000 m
M1	N (cm <sup>-3</sup> )	126.3 ± 70.4	203.5 ± 116.5
	$\sigma$	1.32 ± 0.01	1.35 ± 0.03
	d <sub>p</sub> (nm)	30.5 ± 3.0	23.1 ± 3.5
M2	N (cm <sup>-3</sup> )	211.3 ± 130.1	70.6 ± 51.7
	$\sigma$	1.36 ± 0.02	1.37 ± 0.01
	d <sub>p</sub> (nm)	51.6 ± 5.1	46.7 ± 7.5
M3	N (cm <sup>-3</sup> )	130.4 ± 88.0	45.8 ± 22.6
	$\sigma$	1.37 ± 0	1.37 ± 0.01
	d <sub>p</sub> (nm)	99.7 ± 9.5	94.9 ± 8.7

	N (cm <sup>-3</sup> )	30.9 ± 26.9	9.4 ± 9.5
M4	σ	1.35 ± 0.05	1.31 ± 0.03
	d <sub>p</sub> (nm)	205.4 ± 13.7	207.1 ± 8.5

1

2 b) 11:00 – 17:00

Mode	Parameters	2000 – 3000 m	>3000 m
	N (cm <sup>-3</sup> )	248.1 ± 130.0	155.1 ± 126.0
M1	σ	1.32 ± 0.02	1.34 ± 0.03
	d <sub>p</sub> (nm)	28.6 ± 3.6	24.6 ± 4.8
	N (cm <sup>-3</sup> )	161.8 ± 174.4	83.5 ± 46.9
M2	σ	1.36 ± 0.02	1.37 ± 0.01
	d <sub>p</sub> (nm)	52.4 ± 5.8	49.7 ± 7.4
	N (cm <sup>-3</sup> )	150.8 ± 124.7	67.4 ± 36.0
M3	σ	1.38 ± 0.01	1.37 ± 0.01
	d <sub>p</sub> (nm)	99.7 ± 8.9	97.5 ± 10.0
	N (cm <sup>-3</sup> )	39.0 ± 38.6	17.7 ± 19.4
M4	σ	1.35 ± 0.04	1.32 ± 0.04
	d <sub>p</sub> (nm)	201.9 ± 12.7	224.3 ± 48.4

3

4

5 c) 17:00 – 05:00

Mode	Parameters	2000 – 3000 m	>3000 m
	N (cm <sup>-3</sup> )	224.9 ± 156.7	176.6 ± 117.7
M1	σ	1.32 ± 0.02	1.33 ± 0.03
	d <sub>p</sub> (nm)	27.7 ± 3.1	23.8 ± 3.5

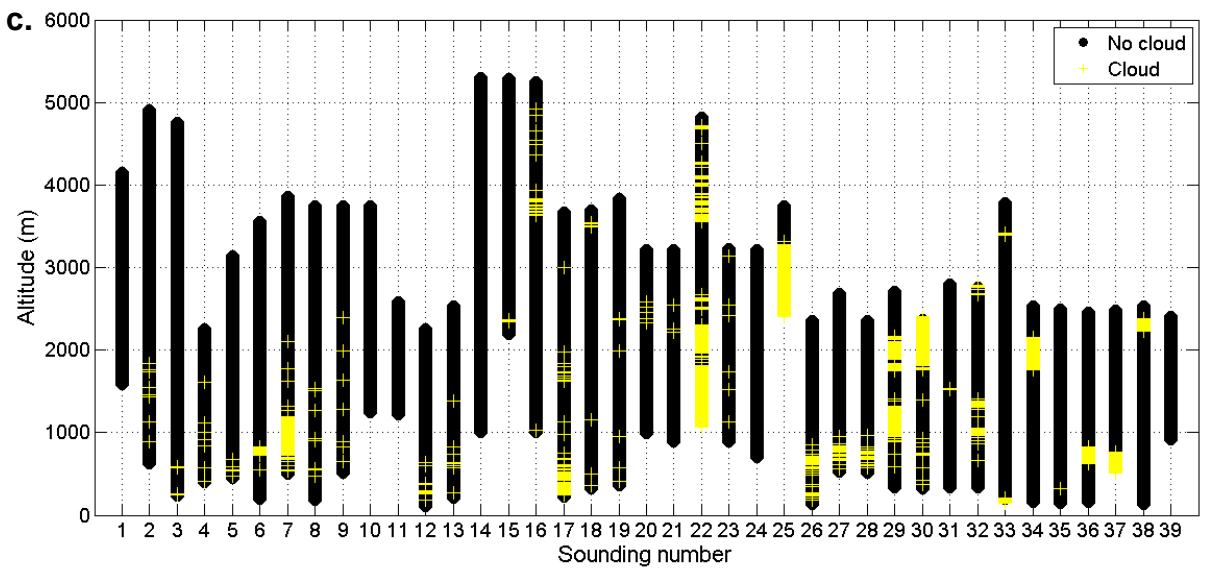
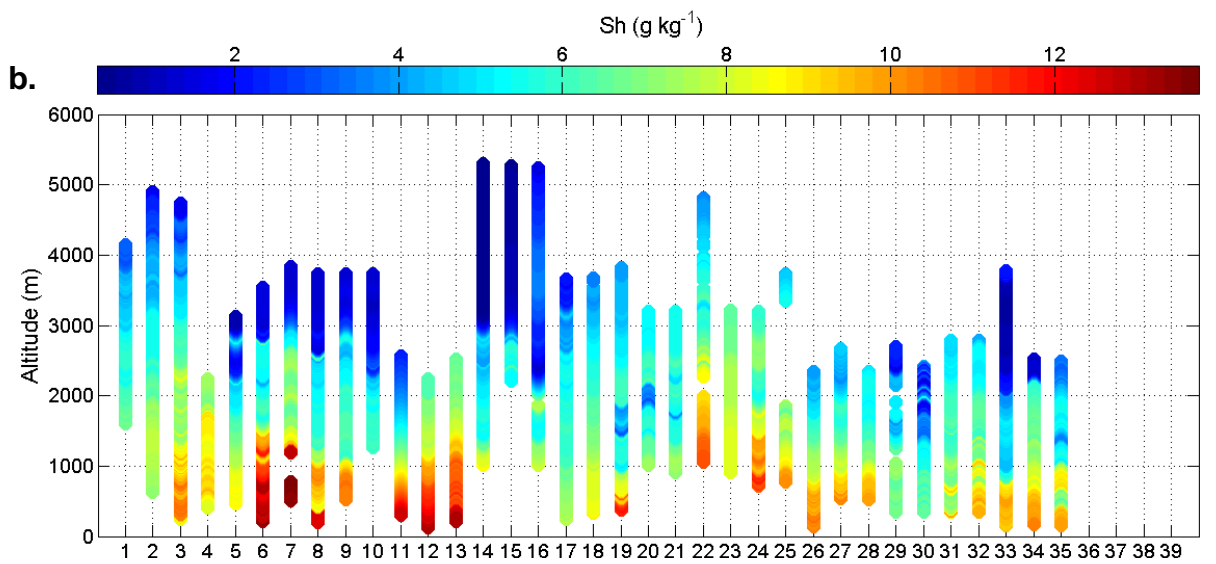
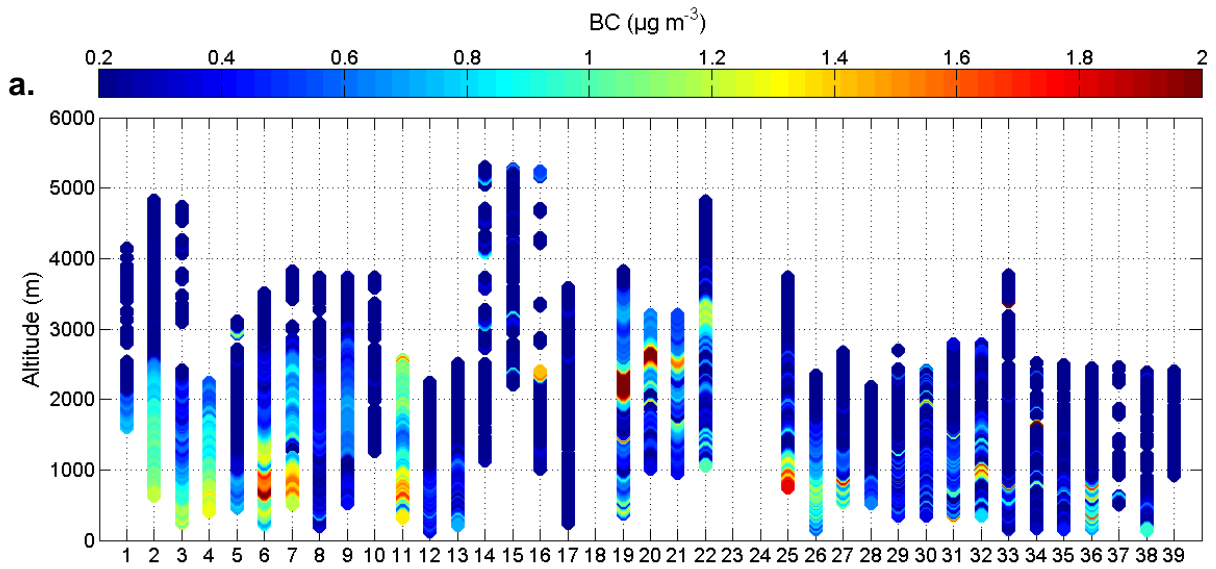
	N (cm <sup>-3</sup> )	227.2 ± 169.4	136.9 ± 9.9
M2	$\sigma$	1.37 ± 0	1.37 ± 0
	d <sub>p</sub> (nm)	50.6 ± 4.1	46.4 ± 5.6
	N (cm <sup>-3</sup> )	167.3 ± 108.7	61.4 ± 58.4
M3	$\sigma$	1.36 ± 0.01	1.35 ± 0.02
	d <sub>p</sub> (nm)	101.6 ± 7.7	102.8 ± 8.4
	N (cm <sup>-3</sup> )	44.7 ± 40.7	9.2 ± 6.2
M4	$\sigma$	1.37 ± 0.05	1.39 ± 0.04
	d <sub>p</sub> (nm)	216.4 ± 17.9	240.3 ± 12.1

1  
2  
3  
4  
5  
6  
7  
8  
9  
10  
11  
12  
13  
14  
15  
16  
17

1

2

3 **Appendix B**



1

2 Fig. B1 Profiles of a. BC, b. specific humidity and c. cloud cover during the ATR-42  
3 soundings performed above the sea.

4

5

## 6 **Acknowledgement**

7 HyMeX SOP1 was supported by CNRS, Météo-France, CNES, IRSTEA, INRA through the  
8 large interdisciplinary international program MISTRALS (Mediterranean Integrated STudies  
9 at Regional And Local Scales) dedicated to the understanding of the Mediterranean Basin  
10 environmental process (<http://www.mistrals-home.org>). We also would like to thank SAFIRE  
11 for their support during instrument integration on the French ATR-42 and HYMEX SOP1  
12 campaign execution. We finally gratefully acknowledge the NOAA Air Resource Laboratory  
13 (ARL) for the provision of the HYSPLIT READY website  
14 (<http://www.arl.noaa.gov/ready.php>) used in this publication for calculating the trajectories.

15

## 16 **References**

17 Asmi, E., Frey, A., Virkkula, A., Ehn, M., Manninen, H. E., Timonen, H., Tolonen-Kivimäki,  
18 O., Aurela, M., Hillamo, R. and Kulmala, M.: Hygroscopicity and chemical composition of  
19 Antarctic sub-micrometre aerosol particles and observations of new particle formation,  
20 *Atmos. Chem. Phys.*, 10(9), 4253–4271, doi:10.5194/acp-10-4253-2010, 2010.

21 Birmili, W., Berresheim, H., Plass-Dülmer, C., Elste, T., Gilge, S., Wiedensohler, A. and  
22 Uhrner, U.: The Hohenpeissenberg aerosol formation experiment (HAFEX): a long-term  
23 study including size-resolved aerosol, H<sub>2</sub>SO<sub>4</sub>, OH, and monoterpenes measurements, *Atmos.*  
24 *Chem. Phys.*, 3(2), 361–376, doi:10.5194/acp-3-361-2003, 2003.

25 Bond, T. C., Anderson, T. L. and Campbell, D.: Calibration and intercomparison of filter-  
26 based measurements of visible light absorption by aerosols, *Aerosol Science & Technology*,  
27 30(6), 582–600, 1999.

28 Boulon, J., Sellegri, K., Hervo, M., Picard, D., Pichon, J.-M., Fréville, P. and Laj, P.:  
29 Investigation of nucleation events vertical extent: a long term study at two different altitude  
30 sites, *Atmos. Chem. Phys.*, 11(12), 5625–5639, doi:10.5194/acp-11-5625-2011, 2011.

31 Boulon, J., Sellegri, K., Venzac, H., Picard, D., Weingartner, E., Wehrle, G., Collaud Coen,  
32 M., Bütikofer, R., Flückiger, E., Baltensperger, U. and Laj, P.: New particle formation and

1 ultrafine charged aerosol climatology at a high altitude site in the Alps (Jungfraujoch, 3580 m  
2 a.s.l., Switzerland), *Atmos. Chem. Phys.*, 10(19), 9333–9349, doi:10.5194/acp-10-9333-2010,  
3 2010.

4 Boy, M., Petäjä, T., Dal Maso, M., Rannik, Ü., Rinne, J., Aalto, P., Laaksonen, A.,  
5 Vaattovaara, P., Joutsensaari, J., Hoffmann, T., Warnke, J., Apostolaki, M., Stephanou, E. G.,  
6 Tsapakis, M., Kouvarakis, A., Pio, C., Carvalho, A., Römpp, A., Moortgat, G., Spirig, C.,  
7 Guenther, A., Greenberg, J., Ciccioli, P. and Kulmala, M.: Overview of the field measurement  
8 campaign in Hyytiälä, August 2001 in the framework of the EU project OSOA, *Atmos.*  
9 *Chem. Phys.*, 4(3), 657–678, doi:10.5194/acp-4-657-2004, 2004.

10 Brock, C. A., Trainer, M., Ryerson, T. B., Neuman, J. A., Parrish, D. D., Holloway, J. S.,  
11 Nicks, D. K., Frost, G. J., Hübler, G., Fehsenfeld, F. C., Wilson, J. C., Reeves, J. M., Lafleur,  
12 B. G., Hilbert, H., Atlas, E. L., Donnelly, S. G., Schauffler, S. M., Stroud, V. R. and  
13 Wiedinmyer, C.: Particle growth in urban and industrial plumes in Texas, *J. Geophys. Res.*,  
14 108(D3), 4111, doi:10.1029/2002JD002746, 2003.

15 Clarke, A. D., Varner, J. L., Eisele, F., Mauldin, R. L., Tanner, D. and Litchy, M.: Particle  
16 production in the remote marine atmosphere: Cloud outflow and subsidence during ACE 1,  
17 *Journal of Geophysical Research: Atmospheres*, 103(D13), 16397–16409,  
18 doi:10.1029/97JD02987, 1998.

19 Crumeyrolle, S., Manninen, H. E., Sellegri, K., Roberts, G., Gomes, L., Kulmala, M., Weigel,  
20 R., Laj, P. and Schwarzenboeck, A.: New particle formation events measured on board the  
21 ATR-42 aircraft during the EUCAARI campaign, *Atmos. Chem. Phys.*, 10(14), 6721–6735,  
22 doi:10.5194/acp-10-6721-2010, 2010.

23 Dall’Osto, M., Querol, X., Alastuey, A., O’Dowd, C., Harrison, R. M., Wenger, J. and  
24 Gómez-Moreno, F. J.: On the spatial distribution and evolution of ultrafine particles in  
25 Barcelona, *Atmos. Chem. Phys.*, 13(2), 741–759, doi:10.5194/acp-13-741-2013, 2013.

26 Draxler, R. R. and Rolph, G. D.: HYSPLIT (Hybrid Single-Particle Lagrangian Integrated  
27 Trajectory) Model access via NOAA ARL READY website  
28 (<http://www.arl.noaa.gov/ready/hysplit4.html>), 2003.

29 Drewnick, F., Hings, S. S., DeCarlo, P., Jayne, J. T., Gonin, M., Fuhrer, K., Weimer, S.,  
30 Jimenez, J. L., Demerjian, K. L., Borrmann, S. and Worsnop, D. R.: A New Time-of-Flight  
31 Aerosol Mass Spectrometer (TOF-AMS)—Instrument Description and First Field

1 Deployment, *Aerosol Science and Technology*, 39(7), 637–658,  
2 doi:10.1080/02786820500182040, 2005.

3 Heintzenberg, J., Covert, D. C. and Van Dingenen, R.: Size distribution and chemical  
4 composition of marine aerosols: a compilation and review, *Tellus B*, 52(4), 1104–1122, 2000.

5 Jeong, C.-H., Hopke, P. K., Chalupa, D. and Utell, M.: Characteristics of Nucleation and  
6 Growth Events of Ultrafine Particles Measured in Rochester, NY, *Environ. Sci. Technol.*,  
7 38(7), 1933–1940, doi:10.1021/es034811p, 2004.

8 Junkermann, W.: An Ultralight Aircraft as Platform for Research in the Lower Troposphere:  
9 System Performance and First Results from Radiation Transfer Studies in Stratiform Aerosol  
10 Layers and Broken Cloud Conditions, *J. Atmos. Oceanic Technol.*, 18(6), 934–946,  
11 doi:10.1175/1520-0426(2001)018<0934:AUAAPF>2.0.CO;2, 2001.

12 Junkermann, W.: The actinic UV-radiation budget during the ESCOMPTE campaign 2001:  
13 results of airborne measurements with the microlight research aircraft D-MIFU, *Atmospheric*  
14 *Research*, 74(1-4), 461–475, doi:10.1016/j.atmosres.2004.06.009, 2005.

15 Kerminen, V.-M., Paramonov, M., Anttila, T., Riipinen, I., Fountoukis, C., Korhonen, H.,  
16 Asmi, E., Laakso, L., Lihavainen, H., Swietlicki, E., Svenningsson, B., Asmi, A., Pandis, S.  
17 N., Kulmala, M. and Petäjä, T.: Cloud condensation nuclei production associated with  
18 atmospheric nucleation: a synthesis based on existing literature and new results, *Atmos.*  
19 *Chem. Phys.*, 12(24), 12037–12059, doi:10.5194/acp-12-12037-2012, 2012.

20 Khosrawi, F. and Konopka, P.: Enhanced particle formation and growth due to mixing  
21 processes in the tropopause region, *Atmospheric Environment*, 37(7), 903–910, 2003.

22 Khosrawi, F., Ström, J., Minikin, A. and Krejci, R.: Particle formation in the Arctic free  
23 troposphere during the ASTAR 2004 campaign: a case study on the influence of vertical  
24 motion on the binary homogeneous nucleation of H<sub>2</sub>SO<sub>4</sub>/H<sub>2</sub>O, *Atmos. Chem. Phys.*, 10(3),  
25 1105–1120, doi:10.5194/acp-10-1105-2010, 2010.

26 Koren, I., Dagan, G. and Altaratz, O.: From aerosol-limited to invigoration of warm  
27 convective clouds, *Science*, 344(6188), 1143–1146, doi:10.1126/science.1252595, 2014.

28 Kristensson, A., Johansson, M., Swietlicki, E., Kivekäs, N., Hussein, T., Nieminen, T.,  
29 Kulmala, M. and Dal Maso, M.: NanoMap: Geographical mapping of atmospheric new

1 particle formation through analysis of particle number size distribution and trajectory data,  
2 Boreal Environ. Res., 19(suppl. B), 2014.

3 Kulmala, M. and Kerminen, V.-M.: On the formation and growth of atmospheric  
4 nanoparticles, Atmospheric Research, 90(2–4), 132–150, doi:10.1016/j.atmosres.2008.01.005,  
5 2008.

6 Kulmala, M., Kontkanen, J., Junninen, H., Lehtipalo, K., Manninen, H. E., Nieminen, T.,  
7 Petäjä, T., Sipilä, M., Schobesberger, S., Rantala, P., Franchin, A., Jokinen, T., Järvinen, E.,  
8 Äijälä, M., Kangasluoma, J., Hakala, J., Aalto, P. P., Paasonen, P., Mikkilä, J., Vanhanen, J.,  
9 Aalto, J., Hakola, H., Makkonen, U., Ruuskanen, T., Mauldin, R. L., Duplissy, J., Vehkamäki,  
10 H., Bäck, J., Kortelainen, A., Riipinen, I., Kurtén, T., Johnston, M. V., Smith, J. N., Ehn, M.,  
11 Mentel, T. F., Lehtinen, K. E. J., Laaksonen, A., Kerminen, V.-M. and Worsnop, D. R.:  
12 Direct Observations of Atmospheric Aerosol Nucleation, Science, 339(6122), 943–946,  
13 doi:10.1126/science.1227385, 2013.

14 Kulmala, M., Vehkamäki, H., Petäjä, T., Dal Maso, M., Lauri, A., Kerminen, V.-M., Birmili,  
15 W. and McMurry, P. H.: Formation and growth rates of ultrafine atmospheric particles: a  
16 review of observations, Journal of Aerosol Science, 35(2), 143–176, 2004.

17 Laakso, L., Grönholm, T., Kulmala, L., Haapanala, S., Hirsikko, A., Lovejoy, E. R., Kazil, J.,  
18 Kurten, T., Boy, M., Nilsson, E. D., Sogachev, A., Riipinen, I., Stratmann, F. and Kulmala,  
19 M.: Hot-air balloon as a platform for boundary layer profile measurements during particle  
20 formation, Boreal environment research, 12(3), 279–294, 2007.

21 Lee, S.-H., Young, L.-H., Benson, D. R., Suni, T., Kulmala, M., Junninen, H., Campos, T. L.,  
22 Rogers, D. C. and Jensen, J.: Observations of nighttime new particle formation in the  
23 troposphere, Journal of Geophysical Research: Atmospheres, 113(D10), n/a–n/a,  
24 doi:10.1029/2007JD009351, 2008.

25 Makkonen, R., Asmi, A., Kerminen, V.-M., Boy, M., Arneth, A., Hari, P. and Kulmala, M.:  
26 Air pollution control and decreasing new particle formation lead to strong climate warming,  
27 Atmos. Chem. Phys., 12(3), 1515–1524, doi:10.5194/acp-12-1515-2012, 2012.

28 Manninen, H. E., Nieminen, T., Asmi, E., Gagné, S., Häkkinen, S., Lehtipalo, K., Aalto, P.,  
29 Vana, M., Mirme, A., Mirme, S., Hörrak, U., Plass-Dülmer, C., Stange, G., Kiss, G., Hoffer,  
30 A., Törö, N., Moerman, M., Henzing, B., de Leeuw, G., Brinkenberg, M., Kouvarakis, G. N.,  
31 Bougiatioti, A., Mihalopoulos, N., O’Dowd, C., Ceburnis, D., Arneth, A., Svenningsson, B.,



1 Swietlicki, E., Tarozzi, L., Decesari, S., Facchini, M. C., Birmili, W., Sonntag, A.,  
2 Wiedensohler, A., Boulon, J., Sellegri, K., Laj, P., Gysel, M., Bukowiecki, N., Weingartner,  
3 E., Wehrle, G., Laaksonen, A., Hamed, A., Joutsensaari, J., Petäjä, T., Kerminen, V.-M. and  
4 Kulmala, M.: EUCAARI ion spectrometer measurements at 12 European sites – analysis of  
5 new particle formation events, *Atmos. Chem. Phys.*, 10(16), 7907–7927, doi:10.5194/acp-10-  
6 7907-2010, 2010.

7 Dal Maso, M., Kulmala, M., Riipinen, I., Wagner, R., Hussein, T., Aalto, P. P. and Lehtinen,  
8 K. E.: Formation and growth of fresh atmospheric aerosols: eight years of aerosol size  
9 distribution data from SMEAR II, Hyytiälä, Finland, *Boreal Environment Research*, 10(5),  
10 323, 2005.

11 Mirme, S., Mirme, A., Minikin, A., Petzold, A., Hörrak, U., Kerminen, V.-M. and Kulmala,  
12 M.: Atmospheric sub-3 nm particles at high altitudes, *Atmos. Chem. Phys.*, 10(2), 437–451,  
13 doi:10.5194/acp-10-437-2010, 2010.

14 Nilsson, E. D. and Kulmala, M.: The potential for atmospheric mixing processes to enhance  
15 the binary nucleation rate, *Journal of Geophysical Research: Atmospheres* (1984–2012),  
16 103(D1), 1381–1389, 1998.

17 O’Dowd, C. D., Geever, M., Hill, M. K., Smith, M. H. and Jennings, S. G.: New particle  
18 formation: Nucleation rates and spatial scales in the clean marine coastal environment,  
19 *Geophysical Research Letters*, 25(10), 1661–1664, 1998.

20 O’Dowd, C. D., Hämeri, K., Mäkelä, J., Väkeva, M., Aalto, P., de Leeuw, G., Kunz, G. J.,  
21 Becker, E., Hansson, H.-C., Allen, A. G., Harrison, R. M., Berresheim, H., Kleefeld, C.,  
22 Geever, M., Jennings, S. G. and Kulmala, M.: Coastal new particle formation: Environmental  
23 conditions and aerosol physicochemical characteristics during nucleation bursts, *Journal of*  
24 *Geophysical Research: Atmospheres*, 107(D19), PAR 12–1–PAR 12–17,  
25 doi:10.1029/2000JD000206, 2002.

26 O’Dowd, C. D. and Leeuw, G. de: Marine aerosol production: a review of the current  
27 knowledge, *Phil. Trans. R. Soc. A*, 365(1856), 1753–1774, doi:10.1098/rsta.2007.2043, 2007.

28 O’Dowd, C. D., Yoon, Y. J., Junkermann, W., Aalto, P., Kulmala, M., Lihavainen, H. and  
29 Viisanen, Y.: Airborne measurements of nucleation mode particles II: boreal forest nucleation  
30 events, *Atmos. Chem. Phys.*, 9(3), 937–944, doi:10.5194/acp-9-937-2009, 2009.

1 Pirjola, L., O'Dowd, C. D., Brooks, I. M. and Kulmala, M.: Can new particle formation occur  
2 in the clean marine boundary layer?, *J. Geophys. Res.*, 105(D21), 26531–26546,  
3 doi:10.1029/2000JD900310, 2000.

4 Rose, C., Sellegri, K., Asmi, E., Hervo, M., Freney, E., Junninen, H., Duplissy, J., Sipilä, M.,  
5 Kontkanen, J., Lehtipalo, K. and Kulmala, M.: Major contribution of neutral clusters to new  
6 particle formation in the free troposphere, *Atmos. Chem. Phys. Discuss.*, 14(12), 18355–  
7 18388, doi:10.5194/acpd-14-18355-2014, 2014.

8 Rose, C., Sellegri, K., Velarde, F., Moreno, I., Ramonet, M., Weinhold, K., Krejci, R.,  
9 Andrade, M., Wiedensohler, A. and Laj, P.: Frequent nucleation events at the high altitude  
10 station of Chacaltaya (5240 m a.s.l.), Bolivia, *Atmospheric Environment*, 102, 18–29,  
11 doi:10.1016/j.atmosenv.2014.11.015, 2015.

12 Rosenfeld, D., Sherwood, S., Wood, R. and Donner, L.: Climate Effects of Aerosol-Cloud  
13 Interactions, *Science*, 343(6169), 379–380, doi:10.1126/science.1247490, 2014.

14 Schobesberger, S., Väänänen, R., Leino, K., Virkkula, A., Backman, J., Pohja, T., Siivola, E.,  
15 Franchin, A., Mikkilä, J., Paramonov, M., Aalto, P. P., Krejci, R., Petäjä, T. and Kulmala, M.:  
16 Airborne measurements over the boreal forest of southern Finland during new particle  
17 formation events in 2009 and 2010, *Boreal environment research*, 18(2), 145–163, 2013.

18 Seidel, D. J., Ao, C. O. and Li, K.: Estimating climatological planetary boundary layer heights  
19 from radiosonde observations: Comparison of methods and uncertainty analysis, *Journal of*  
20 *Geophysical Research: Atmospheres* (1984–2012), 115(D16) [online] Available from:  
21 <http://onlinelibrary.wiley.com/doi/10.1029/2009JD013680/full> (Accessed 4 December 2014),  
22 2010.

23 Sellegri, K., Yoon, Y. J., Jennings, S. G., O'Dowd, C. D., Pirjola, L., Cautenet, S., Chen, H.  
24 and Hoffmann, T.: Quantification of Coastal New Ultra-Fine Particles Formation from In situ  
25 and Chamber Measurements during the BIOFLUX Campaign, *Environ. Chem.*, 2(4), 260–  
26 270, 2005.

27 Sihto, S.-L., Kulmala, M., Kerminen, V.-M., Dal Maso, M., Petäjä, T., Riipinen, I., Korhonen,  
28 H., Arnold, F., Janson, R., Boy, M., Laaksonen, A. and Lehtinen, K. E. J.: Atmospheric  
29 sulphuric acid and aerosol formation: implications from atmospheric measurements for  
30 nucleation and early growth mechanisms, *Atmos. Chem. Phys.*, 6(12), 4079–4091,  
31 doi:10.5194/acp-6-4079-2006, 2006.

1 Suni, T., Kulmala, M., Hirsikko, A., Bergman, T., Laakso, L., Aalto, P. P., Leuning, R.,  
2 Cleugh, H., Zegelin, S., Hughes, D., van Gorsel, E., Kitchen, M., Vana, M., Hörrak, U.,  
3 Mirme, S., Mirme, A., Sevanto, S., Twining, J. and Tardos, C.: Formation and characteristics  
4 of ions and charged aerosol particles in a native Australian Eucalypt forest, *Atmos. Chem.*  
5 *Phys.*, 8(1), 129–139, doi:10.5194/acp-8-129-2008, 2008.

6 Tao, W.-K., Chen, J.-P., Li, Z., Wang, C. and Zhang, C.: Impact of aerosols on convective  
7 clouds and precipitation, *Reviews of Geophysics*, 50(2) [online] Available from:  
8 <http://onlinelibrary.wiley.com/doi/10.1029/2011RG000369/full> (Accessed 20 January 2015),  
9 2012.

10 Tunved, P., Nilsson, E. D., Hansson, H.-C., Ström, J., Kulmala, M., Aalto, P. and Viisanen,  
11 Y.: Aerosol characteristics of air masses in northern Europe: Influences of location, transport,  
12 sinks, and sources, *Journal of Geophysical Research: Atmospheres* (1984–2012), 110(D7)  
13 [online] Available from: <http://onlinelibrary.wiley.com/doi/10.1029/2004JD005085/full>  
14 (Accessed 27 February 2015), 2005.

15 Vaattovaara, P., Huttunen, P. E., Yoon, Y. J., Joutsensaari, J., Lehtinen, K. E. J., O’Dowd, C.  
16 D. and Laaksonen, A.: The composition of nucleation and Aitken modes particles during  
17 coastal nucleation events: evidence for marine secondary organic contribution, *Atmospheric*  
18 *Chemistry and Physics*, 6(12), 4601–4616, 2006.

19 Weber, R. J., Clarke, A. D., Litchy, M., Li, J., Kok, G., Schillawski, R. D. and McMurry, P.  
20 H.: Spurious aerosol measurements when sampling from aircraft in the vicinity of clouds,  
21 *Journal of Geophysical Research*, 103(D21), 28337, doi:10.1029/98JD02086, 1998.

22 Weigel, R., Hermann, M., Curtius, J., Voigt, C., Walter, S., Böttger, T., Lepukhov, B.,  
23 Belyaev, G. and Borrmann, S.: Experimental characterization of the COndensation PArticle  
24 counting System for high altitude aircraft-borne application, *Atmos. Meas. Tech.*, 2(1), 243–  
25 258, doi:10.5194/amt-2-243-2009, 2009.

26 Wiedensohler, A., Cheng, Y. F., Nowak, A., Wehner, B., Achtert, P., Berghof, M., Birmili,  
27 W., Wu, Z. J., Hu, M. and Zhu, T.: Rapid aerosol particle growth and increase of cloud  
28 condensation nucleus activity by secondary aerosol formation and condensation: A case study  
29 for regional air pollution in northeastern China, *Journal of Geophysical Research:*  
30 *Atmospheres* (1984–2012), 114(D2) [online] Available from:

1 <http://onlinelibrary.wiley.com/doi/10.1029/2008JD010884/full> (Accessed 21 February 2014),  
2 2009.

3 Yli-Juuti, T., Nieminen, T., Hirsikko, A., Aalto, P. P., Asmi, E., Hörrak, U., Manninen, H. E.,  
4 Patokoski, J., Dal Maso, M., Petäjä, T., Rinne, J., Kulmala, M. and Riipinen, I.: Growth rates  
5 of nucleation mode particles in Hyytiälä during 2003–2009: variation with particle size,  
6 season, data analysis method and ambient conditions, *Atmos. Chem. Phys.*, 11(24), 12865–  
7 12886, doi:10.5194/acp-11-12865-2011, 2011.

8 Young, L.-H., Benson, D. R., Montanaro, W. M., Lee, S.-H., Pan, L. L., Rogers, D. C.,  
9 Jensen, J., Stith, J. L., Davis, C. A., Campos, T. L., Bowman, K. P., Cooper, W. A. and Lait,  
10 L. R.: Enhanced new particle formation observed in the northern midlatitude tropopause  
11 region, *J. Geophys. Res.*, 112(D10), D10218, doi:10.1029/2006JD008109, 2007.

12

13

14

15

16

17

18

19

20

21

22

23

24

25

26

1 Table 1. Overview of ATR-42 flights performed during the HYMEX campaign between the  
2 11<sup>th</sup> of September and the 4<sup>th</sup> of November 2012 and discussed in the present study. The range  
3 of latitudes (respectively longitudes) corresponds to the minimum and maximum latitudes  
4 (respectively longitudes) reached during the flight. Dominant air mass origins are reported in  
5 the last column according to the following contractions: WE for Western Europe, SMS for  
6 Southern Mediterranean Sea, EMS for Eastern Mediterranean Sea and NE for Northern  
7 Europe.

Date	Take-off – Landing times (UTC)	Flight number	Range of latitudes	Range of longitudes	Dominant air mass origin
12/09/2012	10:10 – 12:51	34	43.5456 – 45.0286	2.8660 – 4.7834	WE
12/09/2012	08:19 – 09:21	35	42.5497 – 43.6403	3.9525 – 9.4847	WE
12/09/2012	10:42 – 14:20	36	42.5390 – 45.4146	7.8651 – 13.4646	WE
12/09/2012	15:22 – 16:49	37	42.5700 – 43.5800	3.9678 – 9.5748	WE
13/09/2012	19:55 – 20:40	38	43.4635 – 43.7027	3.9490 – 4.3397	NE
23/09/2012	14:12 – 17:18	39	42.4688 - 43.5495	3.5163 – 6.6463	WE
26/09/2012	06:09 – 09:32	40	42.2836 – 43.5358	4.0795 – 7.1505	WE
28/09/2012	14:57 – 20:26	41	39.0247 – 43.5556	1.1929 – 4.7809	SMS
02/10/2012	19:43 – 22:11	42	43.5345 – 43.7472	3.9718 – 4.3507	WE
11/10/2012	06:18 – 09:51	43	41.5560 – 43.6521	3.7292 – 6.0734	WE
12/10/2012	01:10 – 04:22	44	40.1657 – 43.6594	3.9816 – 11.6052	WE
12/10/2012	05:43 – 07:05	45	42.6541 – 43.4451	4.2909 – 9.5552	WE
14/10/2012	08:19 – 11:34	46	40.0262 – 43.6537	2.1463 – 7.9019	WE
14/10/2012	13:05 – 15:31	47	39.7553 – 43.5284	4.0702 – 5.3839	SMS
15/10/2012	05:16 – 06:33	48	42.5505 – 43.6523	3.9556 – 9.5761	SMS

15/10/2012	07:47 – 10:59	49	37.9256 – 42.8283	9.4726 – 13.0133	SMS/WE
15/10/2012	12:25 – 13:49	50	42.6096 – 43.5476	4.0322 – 9.5697	North/WE
18/10/2012	15:35 – 19:11	51	41.8076 – 43.5819	3.9640 – 6.6005	SMS
20/10/2012	09:54 – 12:56	52	38.1726 – 43.5235	1.3788 – 4.6854	SMS
20/10/2012	14:14 – 15:19	53	39.7616 – 43.6066	3.9778 – 4.6306	SMS
25/10/012	19:12 – 22:18	54	38.7128 – 43.5761	1.2494 – 4.6609	SMS/WE
26/10/2012	23:25 – 01:24	55	39.8828 – 43.6801	0.2893 – 4.1770	WE
27/10/2012	05:52 – 09:18	56	41.2303 – 43.6439	3.9513 – 7.2013	WE
29/10/2012	14:06 – 16:33	57	43.4495 – 43.7011	3.9438 – 4.3705	NE
30/10/2012	21:41 – 01:16	58	41.2096 – 43.6470	3.9474 – 7.0443	Local
31/10/2012	02:24 – 05:29	59	40.8767 – 43.2733	4.9027 – 10.4004	SMS
03/11/2012	08:01 – 11:35	60	41.9706 – 43.6533	3.9881 – 8.0024	WE
04/11/2012	10:06 – 12:29	61	41.9660 – 43.6798	3.8330 – 8.1176	WE

1

2 Table 2. Nucleation probability and  $N_{5-10}$  concentration (statistics only include  $N_{5-10}$  above the  
3 threshold value) as a function of air mass origin.

Air mass origin	Nucleation probability (%)	$N_{5-10}$ (cm <sup>-3</sup> )		
		Median	25 <sup>th</sup> percentile	75 <sup>th</sup> percentile
Northern Europe	60	343	270	1317
Western Europe	23	315	234	570
Southern Med. Sea	32	361	236	559
Eastern Med. Sea	0.4	531	286	636
Local	10	294	238	326

1  
2  
3  
4  
  
1  
1  
1  
  
13  
14  
15  
16  
  
17  
18  
19  
20  
21  
22  
23  
24  
25  
26

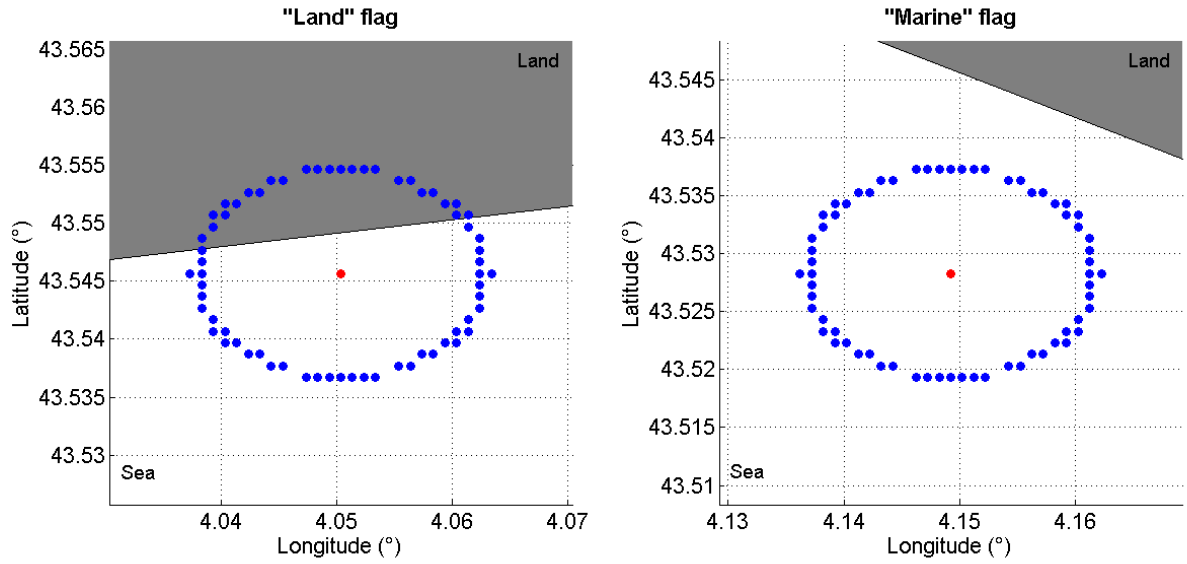


Fig. 1. Method for the determination of the “marine”/“land” flag. The red point corresponds to the location of the aircraft. The blue points represent the  $1000 \pm 50$  m minimum distance from land required for a measurement to be considered as “marine”.

1  
2  
3  
4  
5  
6  
7  
8  
9  
10  
11  
12  
13  
14  
15  
16  
17  
18  
19  
20  
21  
22  
23  
24  
25  
26

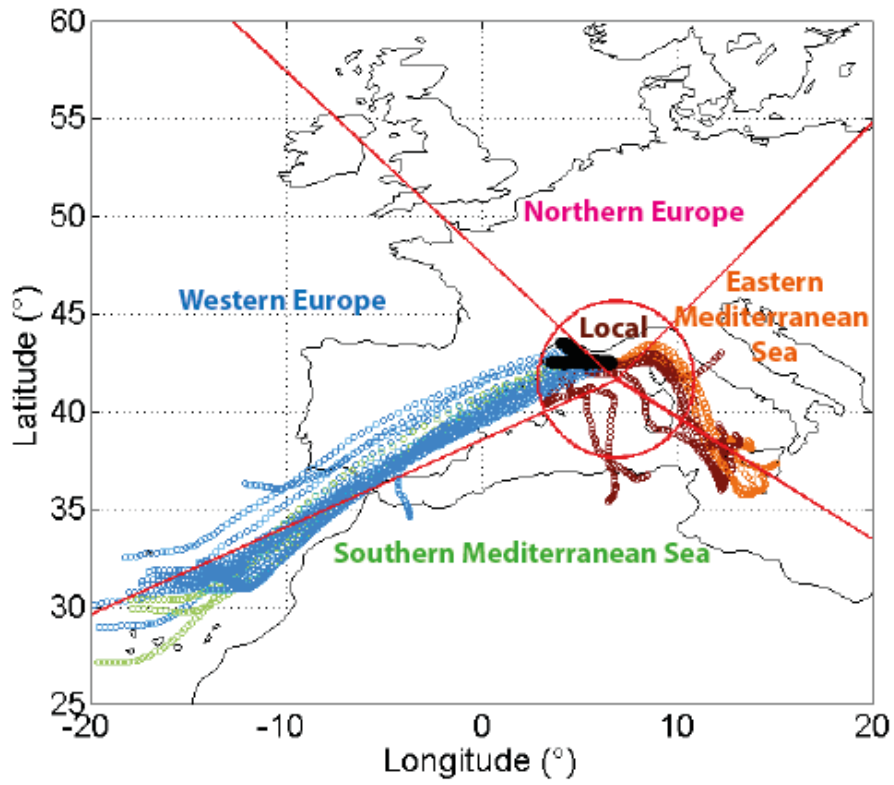


Fig. 2. Illustration of the air mass back trajectories calculation along the flight path (black points) for flight 39 (2012/09/23). The colour coding of the trajectories corresponds to the sectors as given by the text colours.



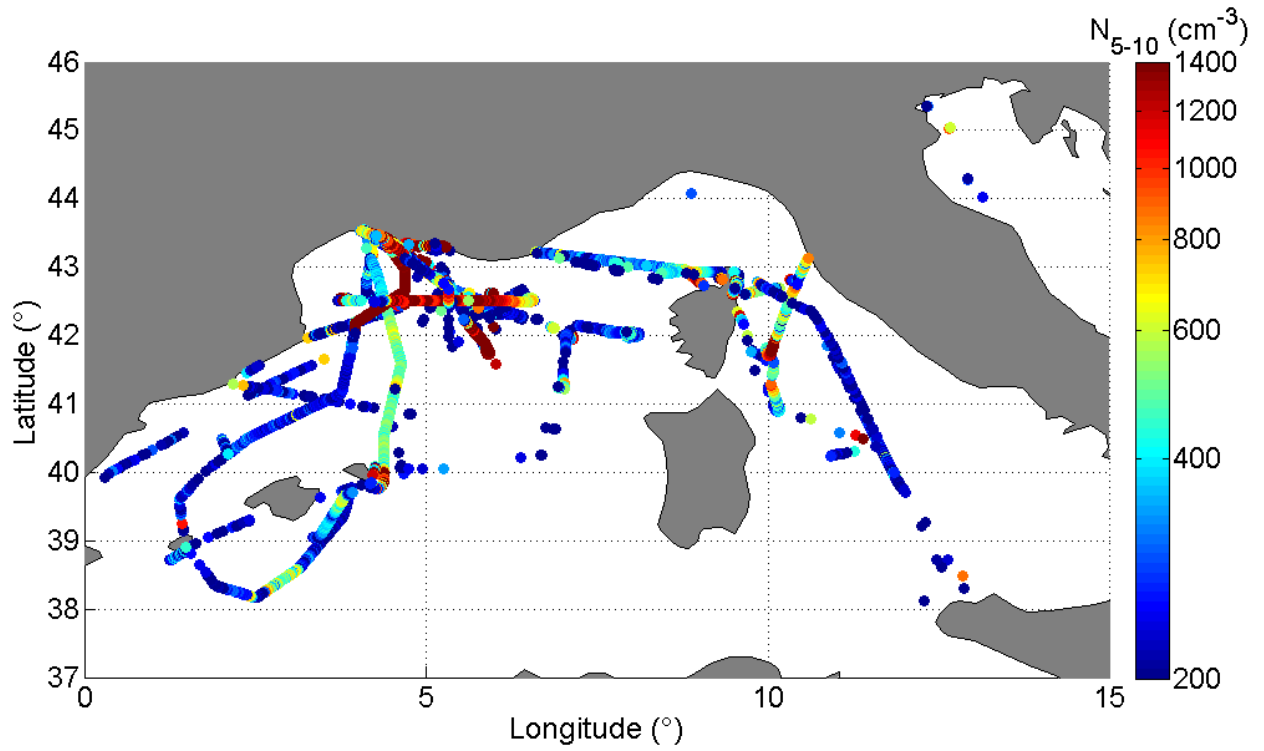


Fig. 3. Location of  $N_{5-10}$  concentrations exceeding the threshold value of  $175 \text{ cm}^{-3}$ . Lower and upper limit of the colour scale were set to the 10<sup>th</sup> and 90<sup>th</sup> percentile of  $N_{5-10}$  concentration, respectively.

1  
2  
11  
12  
13  
14  
15  
16  
17  
18  
19  
20  
21  
22  
23  
24  
25  
26

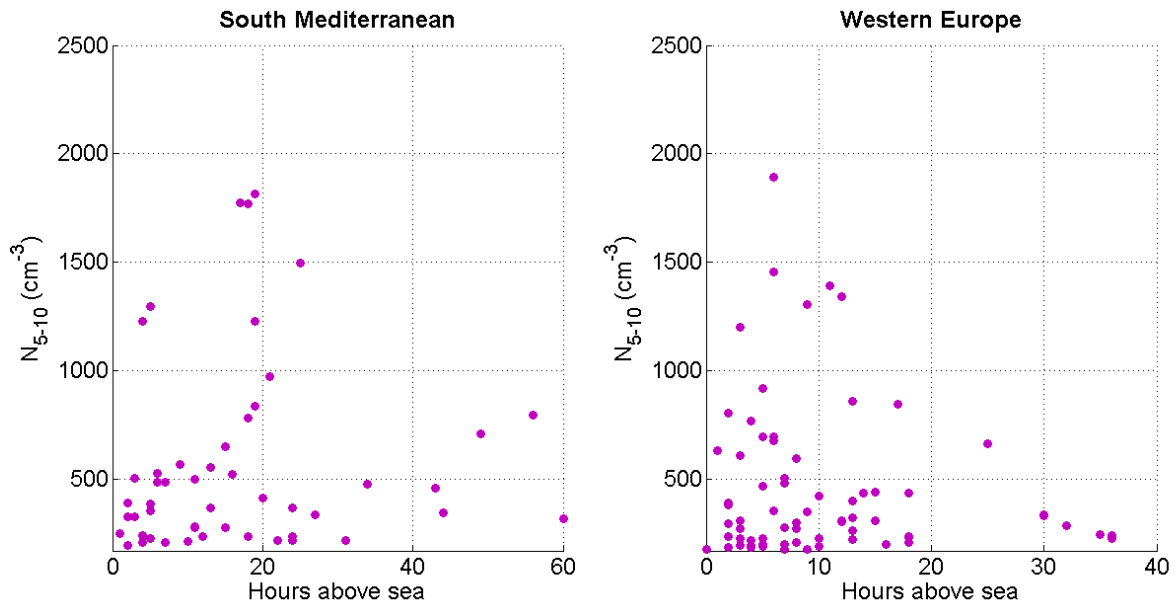
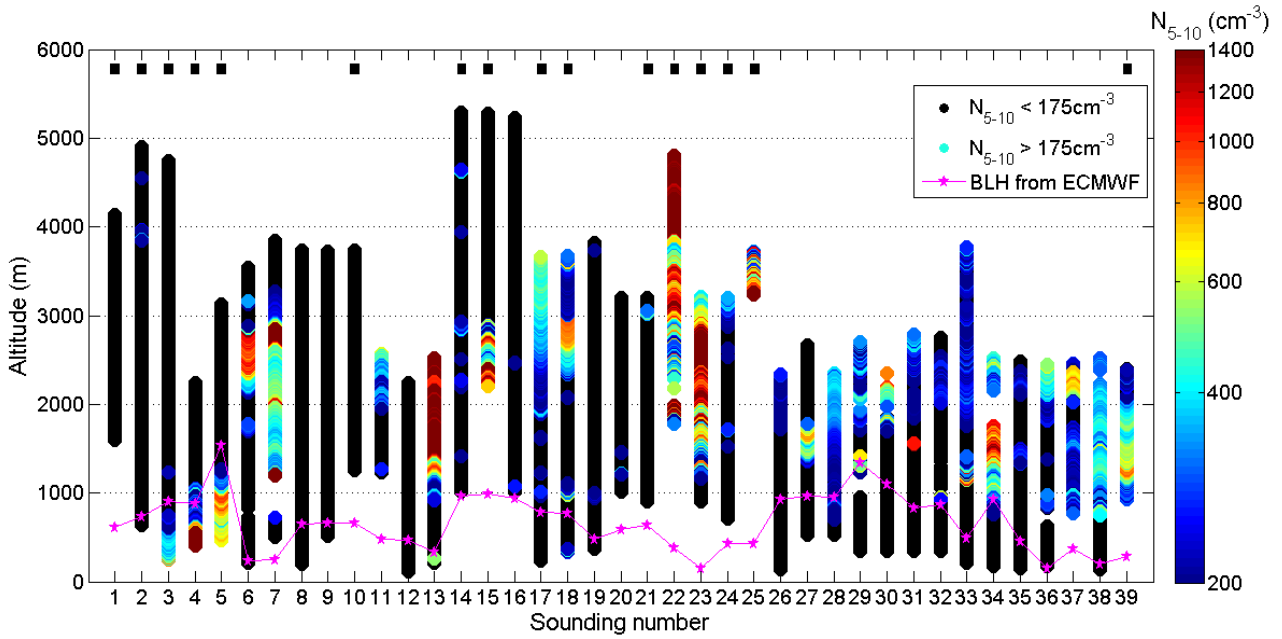


Fig. 4. N<sub>5-10</sub> concentrations as a function of air mass fetch, separately for Southern Mediterranean Sea and Western Europe air masses.

1



1

11 Fig. 5. Profile of the  $N_{5-10}$  concentrations during the ATR-42 soundings performed in clear  
12 sky conditions above the sea. Lower and upper limit of the colour scale were set to the 10<sup>th</sup>  
13 and 90<sup>th</sup> percentile of  $N_{5-10}$  concentration, respectively. Pink stars and line corresponds to the  
14 ECMWF boundary layer height. Black rectangles highlight soundings performed during take-  
15 off or landing phase.

16

17

18

19

20

21

22

23

24

25

26

27

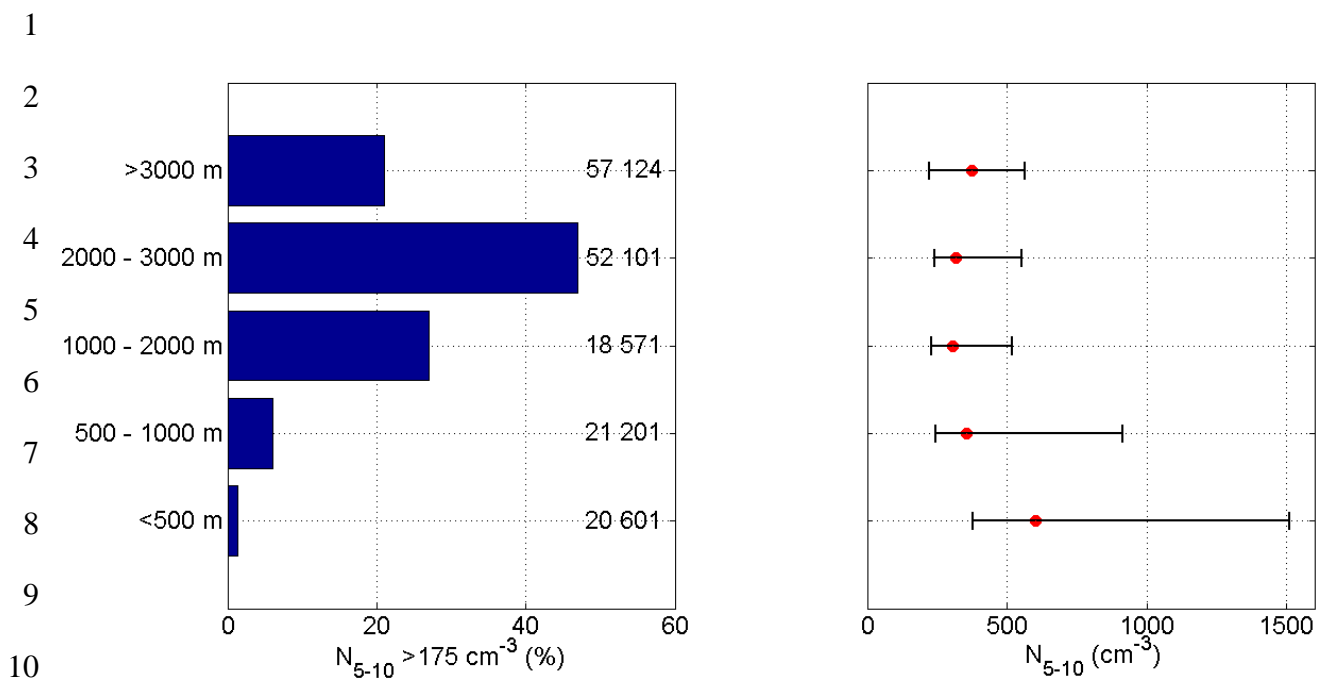
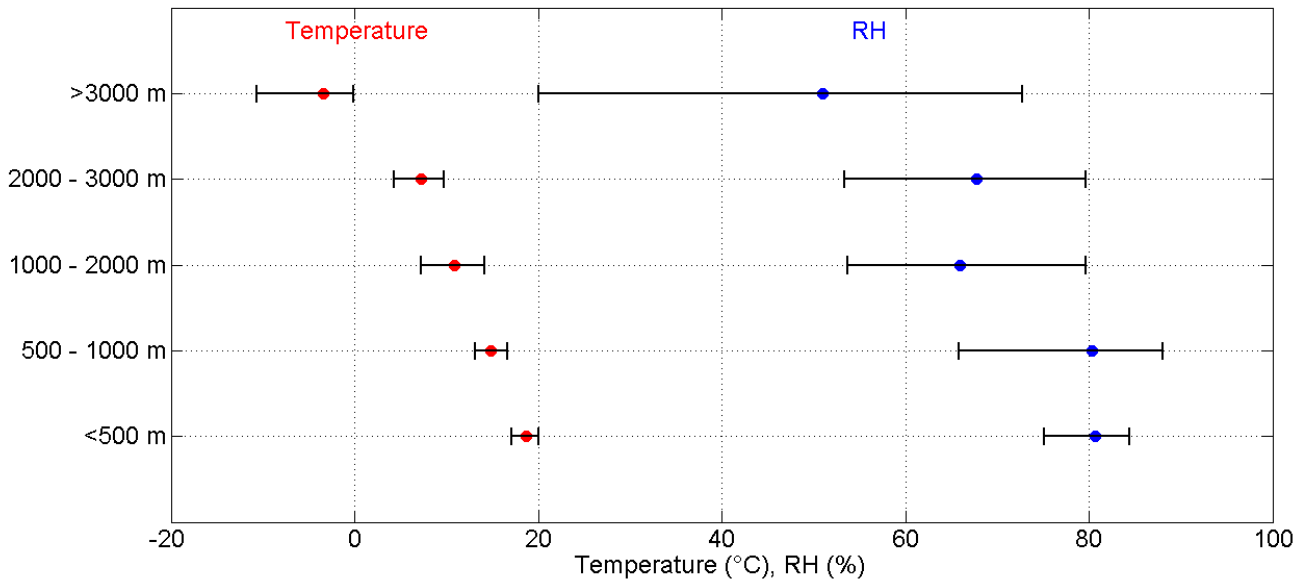


Fig. 6. Statistics on the detection of significant particle concentration in the size range 5 – 10 nm as a function of altitude (left panel, the number of data points is indicated on the plot for each altitude range). Corresponding median concentrations are reported on the right panel; left and right limits of the error bars stand for the 1<sup>st</sup> and 3<sup>rd</sup> quartile, respectively.

1

2



11

12

13 Fig. 7. Median temperature and relative humidity (RH) as a function of altitude range; left and  
14 right limits of the error bars stand for the 1<sup>st</sup> and 3<sup>rd</sup> quartile, respectively.

15

16

17

18

19

20

21

22

23

24

25

26

1  
2  
3  
4  
5  
6  
7  
8  
9  
10  
11  
12  
13  
14  
15  
16  
17  
18  
19  
20  
21  
22  
23  
24  
25  
26

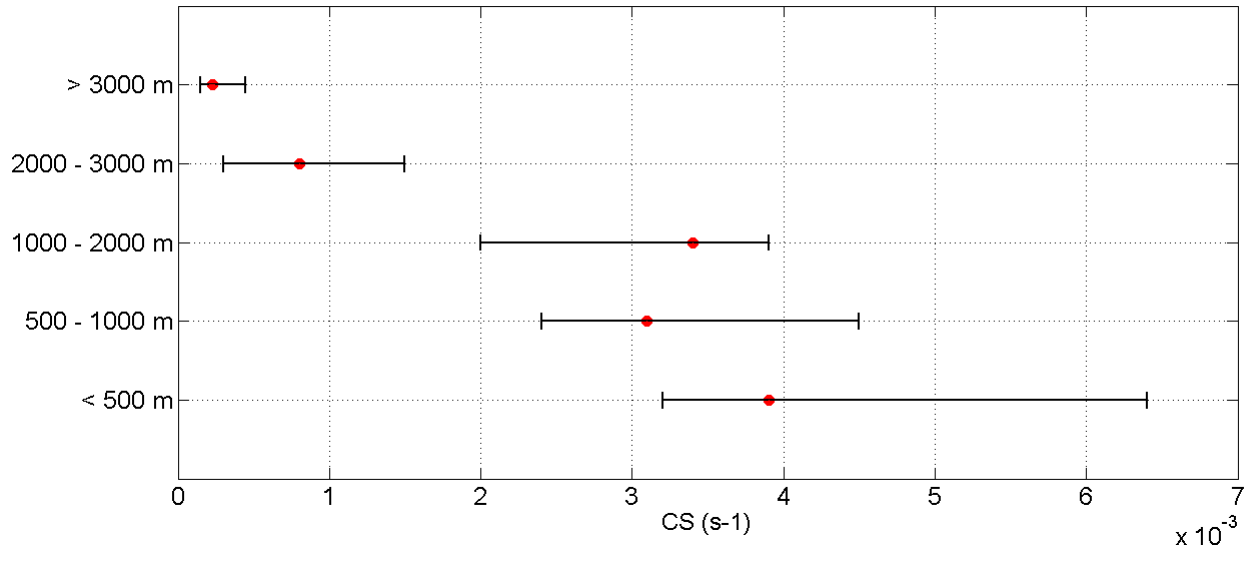


Fig. 8. Median CS as a function of altitude range; left and right limits of the error bars stand for the 1<sup>st</sup> and 3<sup>rd</sup> quartile, respectively. The number of data points included in the statistics is indicated on the plot for each altitude range.

1  
2  
3  
4  
5  
6  
7  
8  
9  
10  
11  
12  
13  
14  
15  
16  
17  
18  
19  
20  
21  
22  
23  
24  
25  
26

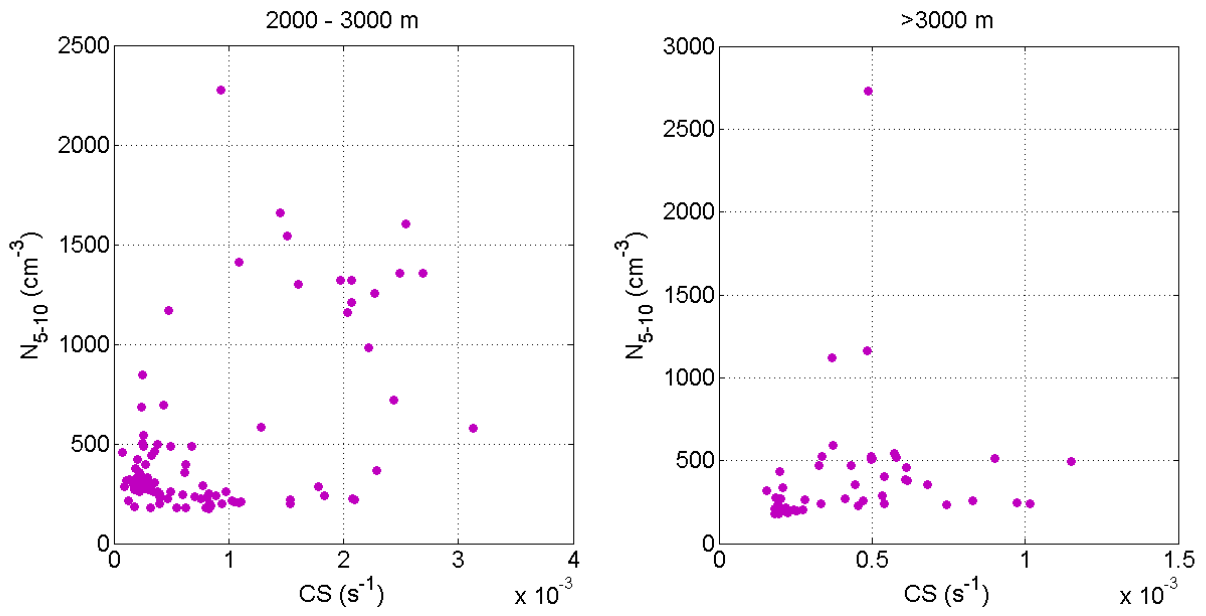


Fig. 9. Particle concentration in the size range 5 – 10 nm as a function of condensation sink (CS) for altitude ranges above 2000 m.

1  
2  
3  
4  
5  
6  
7  
8  
9  
10  
11  
12  
13  
14  
15  
16  
17  
18  
19  
20  
21  
22  
23  
24  
25  
26  
27  
28  
29

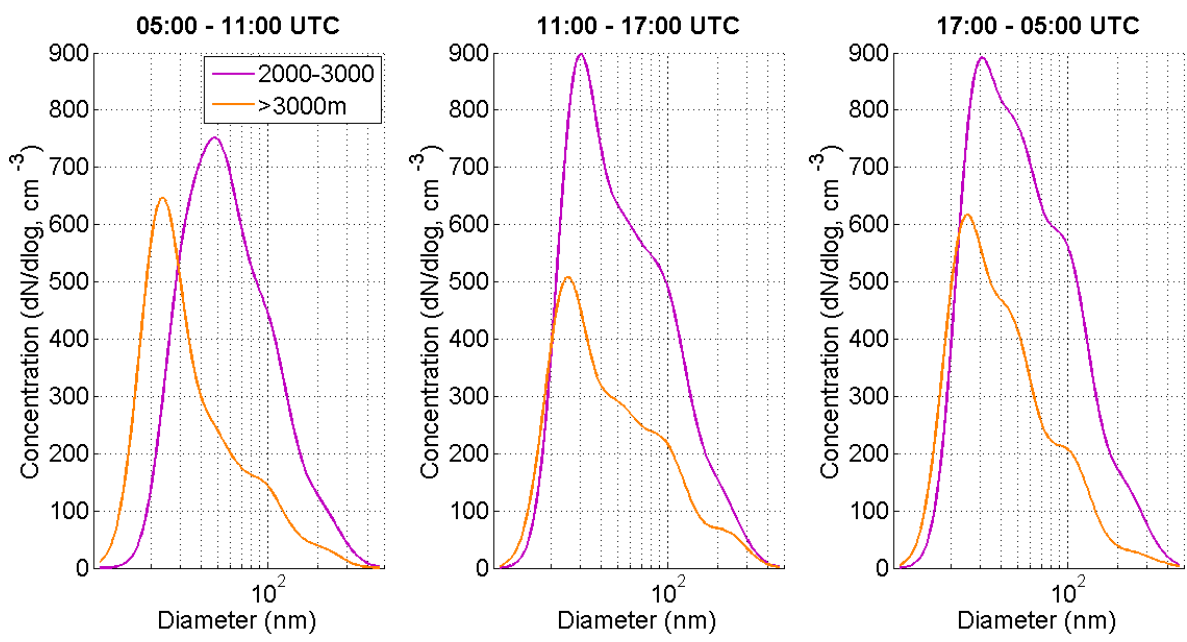


Fig. 10. Averaged fitted SMPS size distributions as a function of daytime and altitude.



1  
2  
3  
4  
5  
6  
7  
8  
9  
10  
11  
12  
13  
14

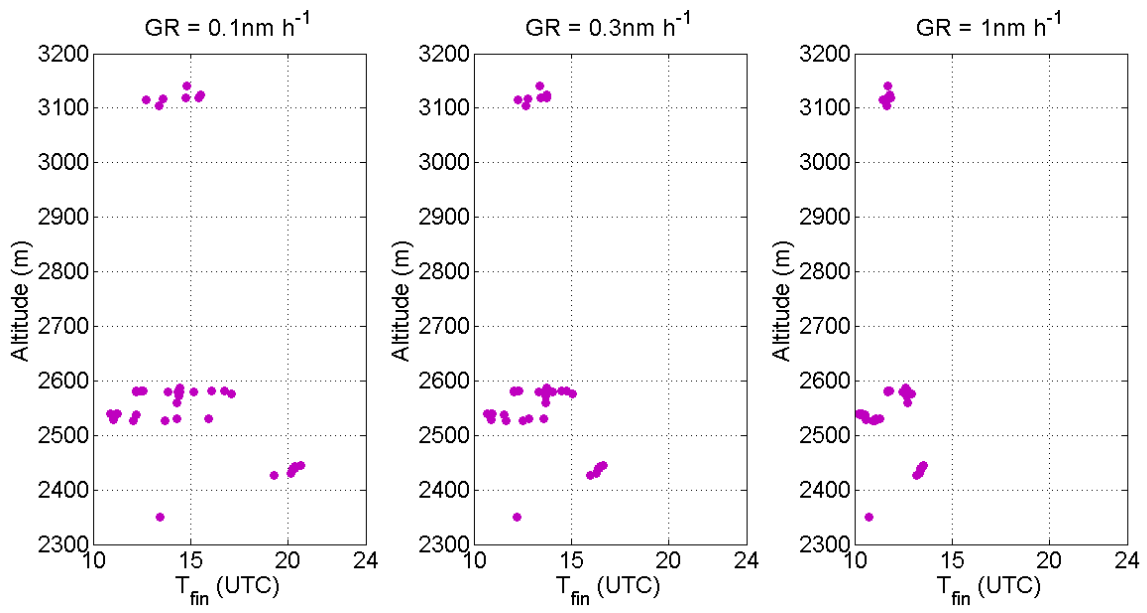


Fig. 11. Estimations of  $t_{fin}$ , the time at which  $N_{5-10}$  concentrations reach half of their initial values, as a function of altitude and particle growth rate.